ColPali: EFFICIENT DOCUMENT RETRIEVAL WITH VISION LANGUAGE MODELS

Manuel Faysse[*1,3] **Hugues Sibille**[*1,4] **Tony Wu**[*1] **Bilel Omrani**[1]
Gautier Viaud[1] **Céline Hudelot**[3] **Pierre Colombo**[2,3]
[1]Illuin Technology [2]Equall.ai [3]CentraleSupélec, Paris-Saclay [4]ETH Zürich
manuel.faysse@centralesupelec.fr

ABSTRACT

Documents are visually rich structures that convey information through text, but also figures, page layouts, tables, or even fonts. Since modern retrieval systems mainly rely on the textual information they extract from document pages to index documents -often through lengthy and brittle processes-, they struggle to exploit key visual cues efficiently. This limits their capabilities in many practical document retrieval applications such as Retrieval Augmented Generation (RAG). To benchmark current systems on visually rich document retrieval, we introduce the Visual Document Retrieval Benchmark *ViDoRe*, composed of various page-level retrieval tasks spanning multiple domains, languages, and practical settings. The inherent complexity and performance shortcomings of modern systems motivate a new concept; doing document retrieval by directly embedding the images of the document pages. We release *ColPali*, a Vision Language Model trained to produce high-quality multi-vector embeddings from images of document pages. Combined with a late interaction matching mechanism, *ColPali* largely outperforms modern document retrieval pipelines while being drastically simpler, faster and end-to-end trainable. We release models, data, code and benchmarks under open licenses at https://huggingface.co/vidore.

1 INTRODUCTION

Document Retrieval consists of matching a user query to relevant documents in a given corpus. It is central to many widespread industrial applications, either as a standalone ranking system (search engines) or as part of more complex information extraction or Retrieval Augmented Generation (RAG) pipelines.

Over recent years, pretrained language models have enabled large improvements in text embedding models. In practical industrial settings, however, the primary performance bottleneck for efficient document retrieval stems not from embedding model performance but from the prior data ingestion pipeline. Indexing a standard PDF document involves several steps. First, PDF parsers or Optical Character Recognition (OCR) systems are used to extract words from the pages. Document layout detection models can then be run to segment paragraphs, titles, and other page objects such as tables, figures, and headers. A chunking strategy is then defined to group text passages with some semantical coherence, and modern retrieval setups may even integrate a captioning step to describe visually rich elements in a natural language form, more suitable for embedding models. In our experiments (Table 2), we typically find that optimizing the ingestion pipeline yields much better performance on visually rich document retrieval than optimizing the text embedding model.

Contribution 1: *ViDoRe*. In this work, we argue that document retrieval systems should not be evaluated solely on the capabilities of text embedding models (Bajaj et al., 2016; Thakur et al., 2021; Muennighoff et al., 2022), but should also consider the context and visual elements of the documents to be retrieved. To this end, we create and openly release *ViDoRe*, a comprehensive benchmark to evaluate systems on page-level document retrieval with a wide coverage of domains, visual elements, and languages. *ViDoRe* addresses practical document retrieval scenarios, where

[*]Equal Contribution

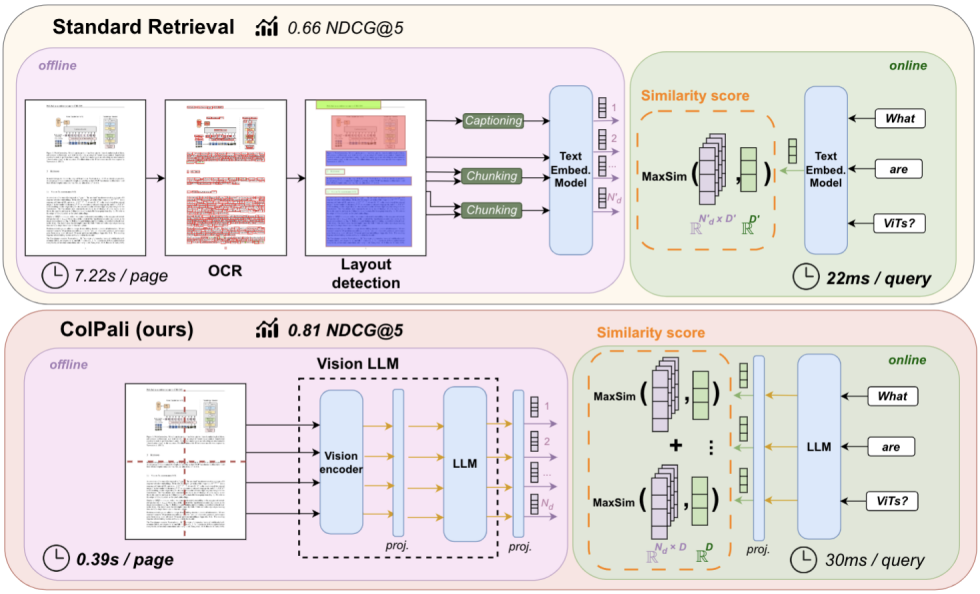

Figure 1: *ColPali* simplifies document retrieval w.r.t. standard retrieval methods while achieving stronger performances with better latencies. Latencies and results are detailed in section 5 and subsection B.4.

queries often necessitate both textual and visual understanding for accurate document matching. We highlight the shortcomings of current text-centric systems in these settings.[1]

Contribution 2: *ColPali*. We propose a novel concept and model architecture based on Vision Language Models (VLMs) to efficiently index documents purely from their visual features, allowing for subsequent fast query matching with late interaction mechanisms (Khattab & Zaharia, 2020). Our method, *ColPali*, significantly outperforms all other retrieval systems on *ViDoRe* while being fast and end-to-end trainable. These results demonstrate the potential and the many benefits of this novel *Retrieval in Vision Space* concept, which could significantly alter the way document retrieval is approached in the industry moving forward. We release all resources at `https://hf.co/vidore`.

2 Problem Formulation & Related Work

Problem Setting. In our setting, a retrieval system scores how relevant a document d from corpus $\mathcal{D}$ is with respect to a query q. Computing the similarity score $s(q, d) \in \mathbb{R}$ for each of the $|\mathcal{D}|$ documents in the corpus creates a ranking we can use to extract the most relevant documents. In this work, we focus on page-level retrieval: *given a query, is the correct document page retrieved by the system?* For coherence with existing literature, we further use the term *document* to refer to individual pages, i.e. the atomic retrieved elements in our setting. As we focus on practical industrial retrieval applications (RAG, search engines) with potentially large corpora sizes, latency constraints are imposed on scoring systems. Most current retrieval systems can be decomposed into (1) an *offline* indexation phase in which a document index is built and (2) an *online* querying phase in which a query is matched to documents from the index and where low latency is vital to the user experience.

Under these industrial constraints, we identify three main properties an efficient document retrieval systems should exhibit: ***(R1) strong retrieval performance****, as measured by standard retrieval metrics;* ***(R2) fast online querying****, measured through average latencies;* ***(R3) high throughput corpus indexation****, ie. the number of pages that can be embedded in a given timeframe.*

[1]The *ViDoRe* benchmark leaderboard is hosted publicly at `https://huggingface.co/spaces/vidore/vidore-leaderboard` to encourage further developments.

2.1 TEXTUAL RETRIEVAL METHODS

Document Retrieval in Text Space. Statistical methods based on word frequency like TF-IDF (Sparck Jones, 1972) and BM25 (Robertson et al., 1994) are still widely used due to their simplicity and efficiency. More recently, neural embedding models based on fine-tuned large language models display state-of-the-art performance on a variety of text embedding tasks and top the retrieval leaderboards (Muennighoff et al., 2022).

Neural Retrievers. In bi-encoder models (Reimers & Gurevych, 2019; Karpukhin et al., 2020; Wang et al., 2022), documents are independently mapped *offline* to a dense vector space. Queries are embedded *online* and matched to documents through a fast cosine distance computation. A slower, but slightly more performant alternative, cross-encoder systems (Wang et al., 2020; Cohere, 2024) concatenate query and document as a single input sequence and iteratively attribute matching scores to each possible combination. This enables full attention computation between query and document terms but comes at the cost of computational efficiency, as $|\mathcal{D}|$ encoding passes must be done online.

Multi-Vector retrieval via late interaction. In the late interaction paradigm introduced by ColBERT (Khattab & Zaharia, 2020), an embedding is pre-computed and indexed per document token. At runtime, similarity can be computed with individual query token embeddings. The idea is to benefit from the rich interaction between individual query and document terms while taking advantage of the offline computation and fast query matching enabled by bi-encoders. See section E for more details.

Retrieval Evaluation. Although benchmarks and leaderboards have been developed to evaluate text embedding models (Thakur et al., 2021; Muennighoff et al., 2022), much of the performance improvements in industrial use cases of embedding models stem from the prior data ingestion pipeline. While documents often rely on visual elements to more efficiently convey information to human readers, text-only systems barely tap into these visual cues. Other work has also independently studied table or chart retrieval systems through repurposed Question Answering datasets (Zhang et al., 2019; Nowak et al., 2024) but only assessing specialized methods for each task.

To our knowledge, no benchmark evaluates document retrieval systems in practical settings; in an end-to-end manner, across several document types and topics, and by evaluating the use of both textual and visual document features.

2.2 INTEGRATING VISUAL FEATURES

Contrastive Vision Language Models. Mapping latent representations of textual content to corresponding representations of visual content has been done by aligning disjoint visual and text encoders through contrastive losses (Radford et al., 2021; Zhai et al., 2023). While some OCR capabilities exist in these models, the visual component is often not optimized for text understanding.

The Fine-grained Interactive Language-Image Pre-training (Yao et al., 2021) framework extends the late interaction mechanism to cross-modal Vision Language Models, relying on max similarity operations between text tokens and image patches.

Visually Rich Document Understanding. To go beyond text, some document-focused models jointly encode text tokens alongside visual or document layout features (Appalaraju et al., 2021; Kim et al., 2021; Huang et al., 2022; Tang et al., 2022). Large Language transformer Models (LLMs) with strong reasoning capabilities have recently been combined with Vision Transformers (ViTs) (Dosovitskiy et al., 2020) to create VLMs (Alayrac et al., 2022; Liu et al., 2023; Bai et al., 2023; Laurençon et al., 2024b) where image patch vectors from contrastively trained ViT models (Zhai et al., 2023) are fed as input embeddings to the LLM and concatenated with the text-token embeddings.

PaliGemma. The PaliGemma-3B model (Beyer et al., 2024) extends concepts from Pali3 (Chen et al., 2023), and projects `SigLIP-So400m/14` (Alabdulmohsin et al., 2023) patch embeddings into Gemma-2B's text vector space (Gemma Team et al., 2024). Along with its reasonable size w.r.t. other performant VLMs, an interesting property of PaliGemma's text model is that it is fine-tuned with full-block attention on the prefix (instruction text and image tokens). See Appendix E for more details.

VLMs display enhanced capabilities in Visual Question Answering, captioning, and document understanding (Yue et al., 2023), but are not optimized for retrieval tasks.

3 THE *ViDoRe* BENCHMARK

Existing benchmarks for contrastive vision-language models primarily evaluate retrieval for natural images (Lin et al., 2014; Borchmann et al., 2021; Thapliyal et al., 2022). On the other hand, textual retrieval benchmarks (Muennighoff et al., 2022) are evaluated at at textual passage level and are not tailored for document retrieval tasks. We fill the gap with *ViDoRe*, a comprehensive benchmark for document retrieval using visual features.

3.1 BENCHMARK DESIGN

ViDoRe is designed to comprehensively evaluate retrieval systems on their capacity to match queries to relevant documents at the page level. This benchmark encompasses multiple orthogonal subtasks, with focuses on various modalities - text, figures, infographics, tables; thematic domains - medical, business, scientific, administrative; or languages - English, French. Tasks also span varying levels of complexity, in order to capture signals from both weaker and stronger systems. As many systems require large amounts of time to index pages (captioning-based approaches can take dozens of seconds per page for instance), we limit the number of candidate documents for each retrieval task in order to evaluate even complex systems in a reasonable timeframe without sacrificing quality. For trainable retrieval systems, we provide a reference training set that can be used to facilitate comparisons.

Dataset	Language	# Queries	# Documents	Description
Academic Tasks				
DocVQA	English	500	500	Scanned documents from UCSF Industry
InfoVQA	English	500	500	Infographics scrapped from the web
TAT-DQA	English	1600	1600	High-quality financial reports
arXiVQA	English	500	500	Scientific Figures from arXiv
TabFQuAD	French	210	210	Tables scrapped from the web
Practical Tasks				
Energy	English	100	1000	Documents about energy
Government	English	100	1000	Administrative documents
Healthcare	English	100	1000	Medical documents
AI	English	100	1000	Scientific documents related to AI
Shift Project	French	100	1000	Environmental reports

Table 1: *ViDoRe* comprehensively evaluates multimodal retrieval methods.

Academic Tasks. We repurpose widely used visual question-answering benchmarks for retrieval tasks: for each page-question-answer triplet, we use the question as the query, and the associated page as the gold document (Table 1). These academic datasets either focus on single specific modalities (Mathew et al., 2020; 2021; Li et al., 2024) or target more varied visually rich documents (Zhu et al., 2022). Moreover, we consider TabFQuAD, a human-labeled dataset on tables extracted from French industrial PDF documents released with this work. Details can be found in subsection A.1.

Practical tasks. We construct topic-specific retrieval benchmarks spanning multiple domains to go beyond repurposed QA datasets and evaluate retrieval in more realistic industrial situations (e.g. RAG). To achieve this, we collect publicly accessible PDF documents and generate queries pertaining to document pages using Claude-3 Sonnet, a high-quality proprietary vision-language model (Anthropic, 2024). In total, we collect 1,000 document pages per topic, which we associate with 100 queries extensively filtered for quality and relevance by human annotators. The corpus topics are intentionally specific to maximize syntactic proximity between documents, creating more challenging retrieval tasks and covering an array of orthogonal domains (Table 1). [2]

Evaluation Metrics. We evaluate performance on our benchmark (Requirement R1) using standard metrics from the retrieval literature (nDCG, Recall@K, MRR). We report nDCG@5 values as the main performance metric in this work and release the complete sets of results along with the models[3].

[2]Answers are generated alongside queries to (1) ground queries and improve their quality and (2) provide resources to foster future work.

[3]`https://huggingface.co/vidore`

To validate compliance with practical industrial requirements (section 2), we also consider query latencies (R2) and indexing throughputs (R3).

3.2 ASSESSING CURRENT SYSTEMS

Unstructured. We evaluate retrieval systems representative of those found in standard industrial RAG pipelines. As is common practice, we rely on the `Unstructured`[4] off-the-shelf tool in the highest resolution settings to construct high-quality text chunks from PDF documents. `Unstructured` orchestrates the document parsing pipeline, relying on deep learning vision models to detect titles and document layouts (Ge et al., 2021), OCR engines (Smith, 2007) to extract text in non-native PDFs, specialized methods or models to detect and reconstruct tables, and implements a chunking strategy (`by-title`) that leverages the detected document structure to preserve section boundaries when concatenating texts. As is common practice, in our simplest `Unstructured` configuration (*text-only*), only textual elements are kept and figures, images, and tables are considered noisy information and are filtered out.

Unstructured + X. While `Unstructured` is a strong baseline by itself, we further augment `Unstructured`'s output by integrating the visual elements. In (+ *OCR*), tables, charts, and images are run through an OCR engine, processed by Unstructured, and chunked independently. In (+ *Captioning*), we set up a fully-fledged captioning strategy (Zhao et al., 2023), in which we feed visual elements to a strong proprietary Vision Language Model (Claude-3 Sonnet (Anthropic, 2024)) to obtain highly detailed textual descriptions of the elements. Both strategies aim to integrate visual elements in the retrieval pipeline but incur significant latency and resource costs (subsection 5.2).

Embedding Model. To embed textual chunks, we evaluate Okapi BM25, the *de facto* standard sparse statistical retrieval method, and the dense encoder of BGE-M3 (Chen et al., 2024), a multilingual neural method with SOTA performance in its size category. Chunks are embedded and scored independently, and page-level scores are obtained by max-pooling over the page's chunk scores.[5]

Contrastive VLMs. We also evaluate the strongest available vision-language embedding models; Jina CLIP (Koukounas et al., 2024), Nomic Embed Vision (Nomic, 2024), and `SigLIP-So400m/14` (Alabdulmohsin et al., 2023).

Results. From a performance perspective, best results are obtained by combining the `Unstructured` parser with visual information, either from captioning strategies or by running OCR on the visual elements (Table 2). Little difference is seen between BM25 and BGE-M3 embeddings highlighting the visual information bottleneck. Contrastive VLMs lag behind. Beyond retrieval performance (R1), the indexing latencies (R2) reported in Figure 2 illustrate that PDF parsing pipelines can be very lengthy, especially when incorporating OCR or captioning strategies. Querying latencies at runtime (R3) are very good for all evaluated systems ($\leq$ 22 ms on a NVIDIA L4) due to fast query encoding and cosine similarity matching.

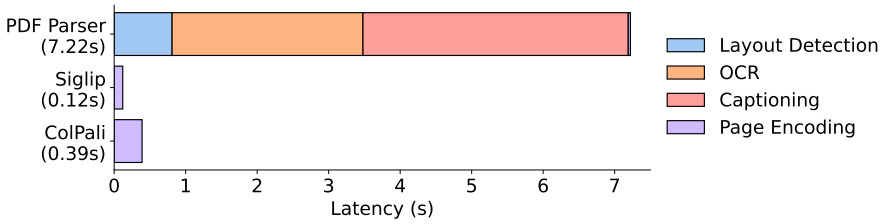

Figure 2: Offline document indexing with *ColPali* is much simpler and faster compared to standard retrieval methods. The PDF Parser results are obtained following the *Unstructured* settings with BGE-M3 detailed in subsection 3.2. All indexing speeds are averaged per-page latencies. More details in subsection B.4

.

[4] `www.unstructured.io`

[5] We empirically validated the max-pooling strategy over sub-page chunks to be more effective than concatenating all page chunks before embedding pagewise.

4 LATE INTERACTION BASED VISION RETRIEVAL

4.1 ARCHITECTURE

Vision-Language Models. Encouraged by their strong document understanding capabilities, we propose adapting recent VLMs for retrieval. The key concept is to leverage the alignment between output embeddings of text and image tokens acquired during multi-modal fine-tuning. To this extent, we introduce *ColPali*, a Paligemma-3B extension that is capable of generating ColBERT-style multi-vector representations of text and images (Figure 1). PaliGemma-3B is a strong candidate due to its small size, the many released checkpoints fine-tuned for different image resolutions and tasks, and the promising performances on various document understanding benchmarks. We add a projection layer to map each of the language model's output token embeddings (whether from text or image tokens) to a vector space of reduced dimension $D = 128$ as used in the ColBERT paper (Khattab & Zaharia, 2020) to keep lightweight bag-of-embedding representations.

Late Interaction. Given query q and document d, we denote as $\mathbf{E_q} \in \mathbb{R}^{N_q \times D}$ and $\mathbf{E_d} \in \mathbb{R}^{N_d \times D}$ their respective multi-vector representation in the common embedding space $\mathbb{R}^D$, where N_q and N_d are respectively the number of vectors in the query and in the document page embeddings. The late interaction operator, $\text{LI}\,(q, d)$, is the sum over all query vectors ${\mathbf{E_q}}^{(i)}$, of its maximum dot product $\langle \cdot | \cdot \rangle$ with each of the N_d document embedding vectors $\mathbf{E_d}_{(1:N_d)}$.

$$\text{LI}\,(q, d) = \sum_{i \in [|1, N_q|]} \max_{j \in [|1, N_d|]} \langle {\mathbf{E_q}}^{(i)} | {\mathbf{E_d}}^{(j)} \rangle \tag{1}$$

Contrastive Loss. The Late Interaction operation is fully differentiable, enabling backpropagation. Let a batch $\{q_k, d_k\}_{k \in [|1,b|]}$ composed of b query-page pairs, where for all $k \in [|1, b|]$, the document page d_k is the document corresponding to query q_k. Following Khattab & Zaharia (2020), we define our in-batch contrastive loss $\mathcal{L}$ as the softmaxed cross-entropy of the positive scores $s_k^+ = \text{LI}\,(q_k, d_k)$ w.r.t. to the maximal in-batch negative scores $s_k^- = \max_{l, l \neq k} \text{LI}\,(q_k, d_l)$[6]:

$$\mathcal{L} = -\frac{1}{b} \sum_{k=1}^{b} \log \left[\frac{\exp\left(s_k^+\right)}{\exp\left(s_k^+\right) + \exp\left(s_k^-\right)} \right] = \frac{1}{b} \sum_{k=1}^{b} \log \left(1 + \exp\left(s_k^- - s_k^+\right)\right) \tag{2}$$

4.2 MODEL TRAINING

Dataset. Our training dataset of 118,695 query-page pairs is comprised of train sets of openly available academic datasets (63%) and a synthetic dataset made up of pages from web-crawled PDF documents and augmented with VLM-generated (Claude-3 Sonnet) pseudo-questions (37%). Dataset split details are given in subsection A.3. Our training set is fully English by design, enabling us to study zero-shot generalization to non-English languages[7]. We explicitly verify no multi-page PDF document is used both *ViDoRe* and in the train set to prevent evaluation contamination. A validation set is created with 2% of the samples to tune hyperparameters. We openly release the training dataset[8] for reproducibility and to encourage further research.

Parameters. All models are trained for 1 epoch on the train set. Unless specified otherwise, we train models in `bfloat16` format, use low-rank adapters (LoRA, Hu et al. (2021)) with $\alpha = 32$ and $r = 32$ on the transformer layers from the language model, as well as the final randomly initialized projection layer, and use a `paged_adamw_8bit` optimizer. We train on an 8 GPU setup with data parallelism, a learning rate of $5e-5$ with linear decay with 2.5% warmup steps, and a batch size of 32.

Query Augmentation. As in Khattab & Zaharia (2020), we append 5 `<unused0>` tokens to the query tokens to serve as a soft, differentiable query expansion or re-weighting mechanism.

[6] We reformulate the loss to leverage the numerically stable `softplus` function where `softplus(x)` $= \log\left(1 + \exp\left(x\right)\right)$

[7] Multilingual data is present in the pretraining corpus of the language model (Gemma-2B) and potentially occurs during PaliGemma-3B's multimodal training.

[8] `https://huggingface.co/datasets/vidore/colpali_train_set`

5 RESULTS

	ArxivQ	DocQ	InfoQ	TabF	TATQ	Shift	AI	Energy	Gov.	Health.	Avg.
`Unstructured` text-only											
- BM25	-	34.1	-	-	44.0	59.6	90.4	78.3	78.8	82.6	-
- BGE-M3	-	28.4$_{\downarrow 5.7}$	-	-	36.1$_{\downarrow 7.9}$	68.5$_{\uparrow 8.9}$	88.4$_{\downarrow 2.0}$	76.8$_{\downarrow 1.5}$	77.7$_{\downarrow 1.1}$	84.6$_{\uparrow 2.0}$	-
`Unstructured` + OCR											
- BM25	31.6	36.8	62.9	46.5	62.7	64.3	92.8	85.9	83.9	87.2	65.5
- BGE-M3	31.4$_{\downarrow 0.2}$	25.7$_{\downarrow 11.1}$	60.1$_{\downarrow 2.8}$	70.8$_{\uparrow 24.3}$	50.5$_{\downarrow 12.2}$	**73.2**$_{\uparrow 8.9}$	90.2$_{\downarrow 2.6}$	83.6$_{\downarrow 2.3}$	84.9$_{\uparrow 1.0}$	91.1$_{\uparrow 3.9}$	66.1$_{\uparrow 0.6}$
`Unstructured` + Captioning											
- BM25	40.1	38.4	70.0	35.4	61.5	60.9	88.0	84.7	82.7	89.2	65.1
- BGE-M3	35.7$_{\downarrow 4.4}$	32.9$_{\downarrow 5.4}$	71.9$_{\uparrow 1.9}$	69.1$_{\uparrow 33.7}$	43.8$_{\downarrow 17.7}$	73.1$_{\uparrow 12.2}$	88.8$_{\uparrow 0.8}$	83.3$_{\downarrow 1.4}$	80.4$_{\downarrow 2.3}$	91.3$_{\uparrow 2.1}$	67.0$_{\uparrow 1.9}$
Contrastive VLMs											
Jina-CLIP	25.4	11.9	35.5	20.2	3.3	3.8	15.2	19.7	21.4	20.8	17.7
Nomic-vision	17.1	10.7	30.1	16.3	2.7	1.1	12.9	10.9	11.4	15.7	12.9
SigLIP (Vanilla)	43.2	30.3	64.1	58.1	26.2	18.7	62.5	65.7	66.1	79.1	51.4
Ours											
SigLIP (Vanilla)	43.2	30.3	64.1	58.1	26.2	18.7	62.5	65.7	66.1	79.1	51.4
BiSigLIP (+fine-tuning)	58.5$_{\uparrow 15.3}$	32.9$_{\uparrow 2.6}$	70.5$_{\uparrow 6.4}$	62.7$_{\uparrow 4.6}$	30.5$_{\uparrow 4.3}$	26.5$_{\uparrow 7.8}$	74.3$_{\uparrow 11.8}$	73.7$_{\uparrow 8.0}$	74.2$_{\uparrow 8.1}$	82.3$_{\uparrow 3.2}$	58.6$_{\uparrow 7.2}$
BiPali (+LLM)	56.5$_{\downarrow -2.0}$	30.0$_{\downarrow -2.9}$	67.4$_{\downarrow -3.1}$	76.9$_{\uparrow 14.2}$	33.4$_{\uparrow 2.9}$	43.7$_{\uparrow 17.2}$	71.2$_{\downarrow -3.1}$	61.9$_{\downarrow -11.7}$	73.8$_{\downarrow -0.4}$	73.6$_{\downarrow -8.8}$	58.8$_{\uparrow 0.2}$
ColPali (+Late Inter.)	**79.1**$_{\uparrow 22.6}$	**54.4**$_{\uparrow 24.5}$	**81.8**$_{\uparrow 14.4}$	**83.9**$_{\uparrow 7.0}$	**65.8**$_{\uparrow 32.4}$	**73.2**$_{\uparrow 29.5}$	**96.2**$_{\uparrow 25.0}$	**91.0**$_{\uparrow 29.1}$	**92.7**$_{\uparrow 18.9}$	**94.4**$_{\uparrow 20.8}$	**81.3**$_{\uparrow 22.5}$

Table 2: **Comprehensive evaluation of baseline models and our proposed method on *ViDoRe*.** Results are presented using nDCG@5 metrics, and illustrate the impact of different components. Text-only metrics are not computed for benchmarks with only visual elements.

5.1 PERFORMANCE (R1)

We show performance is achieved iteratively through the combination of three factors; (1) a carefully crafted task-specific dataset, (2) pairing a pretrained LLM to a vision model to better leverage text semantics from the image, and (3) using multi-vector embeddings rather than a single vector representation to better capture the vast amount of visual information present in a document.

Fine-tuning a Vision Model on a document retrieval oriented dataset: *BiSigLIP*. SigLIP[9] is a strong vision-language bi-encoder producing single vector embeddings, and pretrained on billions of image-text pairs from the English split of WebLI (Chen et al., 2023). Further fine-tuning the textual component of this model on our document-oriented dataset (BiSigLIP) yields clear improvements across the board, particularly on figure retrieval (ArxivQA) and table retrieval tasks (TabFQuAD).

Feeding image patches to a LLM: *BiPali*. In the PaliGemma model architecture, SigLIP-generated patch embeddings are fed to a text language model and we can obtain LLM contextualized output patch embeddings.[10] This technique aligns the image token representations with the text token embeddings in the LLM's embeddings space, and augments the vision model embeddings with the language model's text understanding capabilities. We average pool these representations to obtain a single dense vector, effectively creating a PaliGemma bi-encoder model (BiPali). After fine-tuning on the training dataset, we obtain a model that performs slightly worse in English than the tuned BiSigLIP variant.[11] However, we see notable improvements in French tasks, indicating that BiPali's LLM (Gemma 2B) helps multilingual text understanding. This is particularly notable as our training dataset does not contain non-English samples.

Leveraging Multi-Vector Embeddings through Late Interaction: *ColPali*. One benefit of inputting image patch embeddings through a language model is that they are natively mapped to a latent space similar to the textual input (query). This enables leveraging the ColBERT strategy to construct one

[9] `https://huggingface.co/google/siglip-so400m-patch14-384`

[10] Note that the SigLIP model used in PaliGemma slightly differs in terms of number patches - 1024 patches for PaliGemma's vision encoder, and 729 for the standalone SigLIP model.

[11] This can be explained by the fact that contrary to SigLIP, the original PaliGemma is not trained on contrastive matching tasks, but rather on next token prediction. Our contrastive fine-tuning phase on 119K images to transform PaliGemma into a bi-encoder is 5 orders of magnitude smaller than SigLIP's original contrastive training.

embedding per image patch token, and at inference compute all interactions between text tokens and image patches, resulting in a step-change improvement in performance compared to BiPali. Results in Table 2 show that our *ColPali* model also largely outperforms the strong baselines based on `Unstructured` and captioning, as well as all evaluated text-image embedding models. The difference is particularly stark on the more visually complex benchmark tasks, such as InfographicVQA, ArxivQA, and TabFQuAD, respectively representing infographics, figures, and tables. However, text-centric documents are also better retrieved by the *ColPali* models across all evaluated domains and languages, making our approach the overall best-performing document-retrieval model.

Negative Results. For extensiveness, we also train ColSigLIP, a late interaction variant of the BiSigLIP model but obtain abysmal performances. We attribute this to the large gaps w.r.t. SigLIP's pre-training, in which only a pooled latent representation is used in the contrastive loss, which does not optimize the representations of individual patch and token embeddings. Similarly, we train a BiSigLIP$_{PaliGemma}$ variant, in which we retrieve the image representations from the SigLIP model that has been further updated by PaliGemma fine-tuning, and use the text representations from PaliGemma's text model. After fine-tuning on our dataset, performance is severely inferior to SigLIP$_{Vanilla}$ which simply encodes with SigLIP's original text and vision components. This indicates a logical misalignment between SigLIP embeddings, and Gemma embeddings after PaliGemma training. We detail these results in subsection C.1.

5.2 Latencies & Memory Footprint

Online Querying. (R2) Logically, querying latencies differ between *ColPali* and a BGE-M3 embedding model. For BGE, encoding takes about 22 ms for 15 tokens, while encoding a query with *ColPali*'s language model takes about 30 ms[12]. For smaller corpus sizes, computing the late interaction operation induces marginally small overheads (≈ 1 ms per 1000 pages in the corpus), and the cosine similarity computation between bi-encoder vectors is even faster. Optimized late interaction engines (Santhanam et al., 2022; Lee et al., 2023) enable to easily scale corpus sizes to millions of documents with reduced latency degradations.

Offline Indexing. (R3) Standard retrieval methods using bi-encoders represent each chunk as a single vector embedding, which is easy to store and fast to compute. However, processing a PDF to get the different chunks is the most time-consuming part (layout detection, OCR, chunking), and using captioning to handle multimodal data will only exacerbate this already lengthy process. On the other hand, *ColPali* directly encodes pages from their image representation. Although the model is larger than standard retrieval encoders, skipping the preprocessing allows large speedups at indexing[13] (Figure 2). As pages are embedded end-to-end in single forward pass, the VRAM usage depends exclusively on the sequence length (number of patches per image) which is fixed as well, enabling efficient batching strategies to fully leverage hardware acceleration. ColPali also benefits from most LLM efficiency improvements introduced in the ecosystem such as Flash Attention (Dao, 2023).

Storage Footprint. Our method requires storing a vector per image patch, along with 6 extra text tokens "Describe the image" concatenated to image patches. We project each PaliGemma vector to a lower dimensional space ($D = 128$) to maximize efficiency, leading to a memory footprint of 257.5 KB per page (subsection B.3). Importantly, the memory footprint of the naive ColBERT indexing strategy can be drastically improved through compression and clustering mechanisms (Santhanam et al., 2022; Clavié et al., 2024).

Token pooling. Token pooling (Clavié et al., 2024) is a CRUDE-compliant method (document addition/deletion-friendly) that aims at reducing the sequence length of multi-vector embeddings. For ColPali, many image patches share redundant information, e.g. white background patches. By pooling these patches together, we can reduce the amount of embeddings while retaining most of the page's signal. Retrieval performance with hierarchical mean token pooling on image embeddings is shown in Figure 3 (left). With a pool factor of 3, the total number of vectors is reduced by 66.7% while 97.8% of the original performance is maintained. We note that the Shift dataset—composed of the most text-dense documents—is a clear outlier, showcasing more information dense documents

[12]Computed for a batch size of 1 (online), and averaged over 1000 queries. See subsection B.4

[13]Measures a NVIDIA L4 GPU, averaged on 100 pages, with a batch size of 4 pages for *ColPali* and 8 text chunks for Bi-Encoders. On average, a page is divided into 2.1 chunks. See subsection B.4.

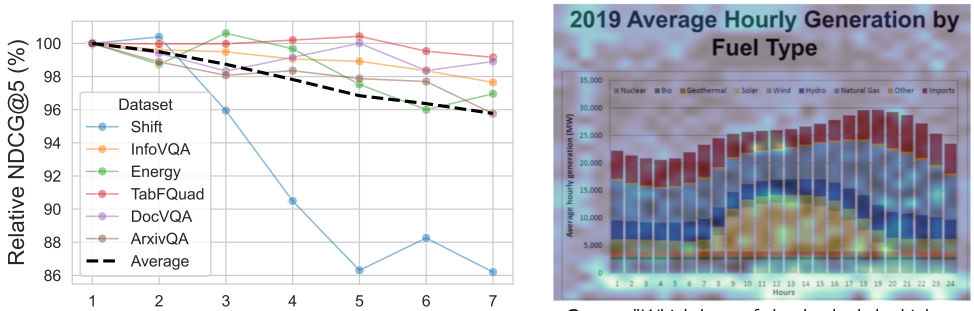

Figure 3: (Left: **Token Pooling**) Relative performance degradation when reducing the number of stored embeddings per document. (Right: **Interpretability**) For each term in a user query, *ColPali* identifies the most relevant document image patches (highlighted zones) and computes a query-to-page matching score.

contain less redundant patches and may be prone to worse performance degradation with such pooling techniques.

5.3 Interpretability

By superimposing the late interaction heatmap on top of the original image, we can visualize the most salient image patches with respect to each term of the query, yielding interpretable insights into model focus zones. As epitomized in Figure 3 (right), we observe *ColPali* exhibits strong OCR capabilities as both the words *"hourly"* and *"hours"* present a high similarity score with the query token <_hour>. We also note particular focus on other non-trivial image features such as the x-axis representing hours being salient. Other visualization examples are shown in Appendix D.

6 Ablation Study

We run various ablations to better understand the mechanisms at play. By default, result deltas reported below refer to nDCG@5 values averaged over all ViDoRe tasks. Detailed results in C.2.

Tradeoffs between model size and the number of image patches. We train a variant of PaliGemma with half the number of image patches (512). While we observe a clear performance degradation with respects to to the 1024-patch *ColPali* model (-24.8 nDCG@5), memory usage is much lower. As an alternative to PaliGemma, we train Idefics2-8B (Laurençon et al., 2024b), a VLM with a similar architecture and based on a Mistral-7B (Jiang et al., 2023) language backbone and a SigLIP vision encoder paired with a perceiver resampler. The most notable differences with PaliGemma lie in the size of the language model (2B and 7B resp.) and the number of image patches (between 512 and 2048 for PaliGemma, and 64 post-resampling for Idefics2[14]). Our results suggest better language models enable more efficient representations of image embeddings - ColIdefics2 with 64 patches largely outperforms out *ColPali* with 512 patches (+20.1 nDCG@5). However ColIdefics2 (64) remains less accurate than ColPali (1024) (-4.7 nDCG@5) while being about twice as slow in terms of training and inference latency. These results suggest there are *tradeoffs* between performance (R1), latencies during online querying (R2) and offline indexation phases (R3), and index memory size.

Unfreezing the vision component. We train a *ColPali* variant by also backpropagating through and updating the vision encoder and the projection layer. This leads to a slight performance degradation (-0.7 nDCG@5). These conclusions may change with larger scales of training data.

Impact of "query augmentation" tokens. In ColBERT, special tokens are concatenated to the input query to serve as soft query augmentation buffers. Training without these tokens, we observe no significant performance difference in the English benchmarks. However, performance on the French tasks seems to improve ($+9.8$ nDCG@G on Shift, $+6.3$ nDCG@5 on TabFQuAD, Table 7).

[14]With the option of adding 4 sub-image crops of 64 tokens each to the sequence, for a total of 320 tokens

Impact of the Pairwise CE loss. Training with an in-batch negative contrastive loss, instead of the pairwise CE loss that only considers the hardest negative sample, leads to a slight performance degradation (-1.6 nDCG@5) on the aggregated benchmark.

Adapting models to new tasks. Contrary to more complex multi-step retrieval pipelines, *ColPali* can be trained end-to-end, directly optimizing the downstream retrieval task which greatly facilitates fine-tuning to boost performance on specialized domains, multilingual retrieval, or specific visual elements the model struggles with. To demonstrate, we add 1552 samples representing French tables and associated queries to the training set. This represents the only French data in the training set, with all other examples being kept unchanged. We see clear nDCG@5 improvements ($+2.6$) and even starker Recall@1 gains ($+5$) on the TabFQuAD benchmark, with no performance degradation on the rest of the benchmark tasks ($+0.4$ nDCG@5 overall).

Better VLMs lead to better visual retrievers. As improved VLMs are released, it is interesting to observe if improved performances on generative tasks translate once these models are adapted for image retrieval tasks through ColPali training strategies. We train the recently released Qwen2-VL 2B (Wang et al., 2024b), a SOTA 2 billion parameter generative VLM, with the same data and training strategy, obtaining ColQwen2-VL. To approximately match ColPali's memory requirements, we limit the number of image patches to 768, slightly less than ColPali's 1024 patches. We observe clear performance improvements of $+5.3$ nDCG@5 values over ColPali showcasing clear performance correlations between generative benchmarks performance and retrieving metrics.

Out-of-domain generalization. Some of the datasets in the ViDoRe benchmark have train sets, which we have integrated within the ColPali train set (eg. academic tasks). This is standard in embedding models (Wang et al., 2024a; Lee et al., 2024), and while ColPali also exhibits strong performance on tasks in which this is not the case (French data is never seen by the model during training for instance), it remains interesting to evaluate model performance when training is done on a fully disjoint data distribution. We train a ColPali variant solely using the recent DocMatix dataset (Laurençon et al., 2024a), a large scale, synthetically annotated visual document question answering dataset, which we subsample to obtain a comparably-sized train set. Results on ViDoRe show the performance drop is minor (-2.2 nDCG@5), still outperforming the closest baseline method by over 12 points. These results showcase ColPali generalizes well outside of its training distribution, and demonstrate that our results are not unreasonably boosted with respect to baselines (BGE-M3) that cannot be fine-tuned on the same data[15]

7 Conclusions

In this work, we introduced the Visual Document Retrieval Benchmark (*ViDoRe*), which evaluates document retrieval systems in realistic settings involving visually complex documents. We demonstrated that current retrieval pipelines and contrastive vision-language models struggle to efficiently exploit visual information embedded in documents, leading to suboptimal performance. To address this, we presented *ColPali*, a novel retrieval method that leverages Vision-Language Models to create high-quality, multi-vector embeddings purely from visual document features. *ColPali* largely outperforms the best existing document retrieval methods while enabling faster corpus indexing times and maintaining low querying latencies, thus circumventing many pain points of modern document retrieval applications. We hope to drive industrial adoption, and to encourage future work by publicly releasing the *ViDoRe* benchmark, the data, the codebase, and all models and baselines from our work.

Future Work. Beyond performance improvements that could be obtained through better data, backbone models or training strategies, our vision at term is to combine visual retrieval systems and visually grounded query answering to create end-to-end RAG systems that purely function from image features. This idea is supported by concurrent work (Ma et al., 2024) showcasing the strong promises of VLMs for visual QA, and may eventually become a new industrial standard for document processing. In this line of work, reliability is key, and confidence estimation techniques for Information Retrieval methods could become central to implement abstention mechanisms (Gisserot-Boukhlef et al., 2024), and are particularly interesting given the information rich multi-vector scoring

[15]To train with data resembling the one BGE-M3 models would see at inference time would require running complex extraction pipelines for the more than 100K documents in the training set, notably relying on external proprietary captioning models which is both too costly and lengthy. This is not needed to train vision-based models.

mechanisms of late interaction systems. Expanding benchmarking efforts to cover more languages, modalities, and tasks is also a crucial future research direction (Jiang et al., 2024).

REPRODUCIBILITY STATEMENT

For transparency, reproducibility and to foster future work, we release our training data, model checkpoints (adapters), entire codebase, and complete evaluation benchmark under MIT licenses as detailed in the main paper. We also host a public *ViDoRe* leaderboard[16] to foster concurrent work in the space. The supplementary material further details training configurations for our models (also specified in HuggingFace model repositories), and dives into the process we used to generate synthetic data, how latency computations are performed, as well as provides further detailed evaluation results.

REFERENCES

Ibrahim Alabdulmohsin, Xiaohua Zhai, Alexander Kolesnikov, and Lucas Beyer. Getting ViT in Shape: Scaling Laws for Compute-Optimal Model Design. 2023. doi: 10.48550/ARXIV.2305.13035. URL https://arxiv.org/abs/2305.13035. Publisher: arXiv Version Number: 5.

Jean-Baptiste Alayrac, Jeff Donahue, Pauline Luc, Antoine Miech, Iain Barr, Yana Hasson, Karel Lenc, Arthur Mensch, Katie Millican, Malcolm Reynolds, Roman Ring, Eliza Rutherford, Serkan Cabi, Tengda Han, Zhitao Gong, Sina Samangooei, Marianne Monteiro, Jacob Menick, Sebastian Borgeaud, Andrew Brock, Aida Nematzadeh, Sahand Sharifzadeh, Mikolaj Binkowski, Ricardo Barreira, Oriol Vinyals, Andrew Zisserman, and Karen Simonyan. Flamingo: a Visual Language Model for Few-Shot Learning. 2022. doi: 10.48550/ARXIV.2204.14198. URL https://arxiv.org/abs/2204.14198. Publisher: arXiv Version Number: 2.

Anthropic. The Claude 3 Model Family: Opus, Sonnet, Haiku, 2024. URL https://www-cdn.anthropic.com/de8ba9b01c9ab7cbabf5c33b80b7bbc618857627/Model_Card_Claude_3.pdf.

Srikar Appalaraju, Bhavan Jasani, Bhargava Urala Kota, Yusheng Xie, and R. Manmatha. DocFormer: End-to-End Transformer for Document Understanding, 2021. URL https://arxiv.org/abs/2106.11539. Version Number: 2.

Jinze Bai, Shuai Bai, Shusheng Yang, Shijie Wang, Sinan Tan, Peng Wang, Junyang Lin, Chang Zhou, and Jingren Zhou. Qwen-VL: A Versatile Vision-Language Model for Understanding, Localization, Text Reading, and Beyond. 2023. doi: 10.48550/ARXIV.2308.12966. URL https://arxiv.org/abs/2308.12966. Publisher: arXiv Version Number: 3.

Payal Bajaj, Daniel Campos, Nick Craswell, Li Deng, Jianfeng Gao, Xiaodong Liu, Rangan Majumder, Andrew McNamara, Bhaskar Mitra, Tri Nguyen, Mir Rosenberg, Xia Song, Alina Stoica, Saurabh Tiwary, and Tong Wang. MS MARCO: A Human Generated MAchine Reading COmprehension Dataset, 2016. URL https://arxiv.org/abs/1611.09268. Version Number: 3.

Lucas Beyer, Andreas Steiner, André Susano Pinto, Alexander Kolesnikov, Xiao Wang, Daniel Salz, Maxim Neumann, Ibrahim Alabdulmohsin, Michael Tschannen, Emanuele Bugliarello, Thomas Unterthiner, Daniel Keysers, Skanda Koppula, Fangyu Liu, Adam Grycner, Alexey Gritsenko, Neil Houlsby, Manoj Kumar, Keran Rong, Julian Eisenschlos, Rishabh Kabra, Matthias Bauer, Matko Bošnjak, Xi Chen, Matthias Minderer, Paul Voigtlaender, Ioana Bica, Ivana Balazevic, Joan Puigcerver, Pinelopi Papalampidi, Olivier Henaff, Xi Xiong, Radu Soricut, Jeremiah Harmsen, and Xiaohua Zhai. Paligemma: A versatile 3b vlm for transfer, 2024. URL https://arxiv.org/abs/2407.07726.

Burton H. Bloom. Space/time trade-offs in hash coding with allowable errors. *Commun. ACM*, 13(7): 422–426, July 1970. ISSN 0001-0782. doi: 10.1145/362686.362692. URL https://doi.org/10.1145/362686.362692. Place: New York, NY, USA Publisher: Association for Computing Machinery.

[16] https://huggingface.co/spaces/vidore/vidore-leaderboard

Łukasz Borchmann, Michał Pietruszka, Tomasz Stanislawek, Dawid Jurkiewicz, Michał Turski, Karolina Szyndler, and Filip Graliński. DUE: End-to-End Document Understanding Benchmark. In *Thirty-fifth Conference on Neural Information Processing Systems Datasets and Benchmarks Track (Round 2)*, 2021. URL https://openreview.net/forum?id=rNs2FvJGDK.

Jianlv Chen, Shitao Xiao, Peitian Zhang, Kun Luo, Defu Lian, and Zheng Liu. BGE M3-Embedding: Multi-Lingual, Multi-Functionality, Multi-Granularity Text Embeddings Through Self-Knowledge Distillation, 2024. URL https://arxiv.org/abs/2402.03216. Version Number: 3.

Xi Chen, Xiao Wang, Lucas Beyer, Alexander Kolesnikov, Jialin Wu, Paul Voigtlaender, Basil Mustafa, Sebastian Goodman, Ibrahim Alabdulmohsin, Piotr Padlewski, Daniel Salz, Xi Xiong, Daniel Vlasic, Filip Pavetic, Keran Rong, Tianli Yu, Daniel Keysers, Xiaohua Zhai, and Radu Soricut. PaLI-3 Vision Language Models: Smaller, Faster, Stronger, 2023. URL https://arxiv.org/abs/2310.09199. Version Number: 2.

Benjamin Clavié, Antoine Chaffin, and Griffin Adams. Reducing the Footprint of Multi-Vector Retrieval with Minimal Performance Impact via Token Pooling, 2024. URL https://arxiv.org/abs/2409.14683. Version Number: 1.

Cohere. Introducing Rerank 3: A New Foundation Model for Efficient Enterprise Search & Retrieval, April 2024. URL https://cohere.com/blog/rerank-3.

Tri Dao. Flashattention-2: Faster attention with better parallelism and work partitioning, 2023. URL https://arxiv.org/abs/2307.08691.

Timothée Darcet, Maxime Oquab, Julien Mairal, and Piotr Bojanowski. Vision Transformers Need Registers. 2023. doi: 10.48550/ARXIV.2309.16588. URL https://arxiv.org/abs/2309.16588. Publisher: [object Object] Version Number: 2.

Jacob Devlin, Ming-Wei Chang, Kenton Lee, and Kristina Toutanova. BERT: Pre-training of Deep Bidirectional Transformers for Language Understanding, 2018. URL https://arxiv.org/abs/1810.04805. Version Number: 2.

Alexey Dosovitskiy, Lucas Beyer, Alexander Kolesnikov, Dirk Weissenborn, Xiaohua Zhai, Thomas Unterthiner, Mostafa Dehghani, Matthias Minderer, Georg Heigold, Sylvain Gelly, Jakob Uszkoreit, and Neil Houlsby. An Image is Worth 16x16 Words: Transformers for Image Recognition at Scale. 2020. doi: 10.48550/ARXIV.2010.11929. URL https://arxiv.org/abs/2010.11929. Publisher: arXiv Version Number: 2.

Zheng Ge, Songtao Liu, Feng Wang, Zeming Li, and Jian Sun. YOLOX: Exceeding YOLO Series in 2021, 2021. URL https://arxiv.org/abs/2107.08430. Version Number: 2.

Gemma Team, Thomas Mesnard, Cassidy Hardin, Robert Dadashi, Surya Bhupatiraju, Shreya Pathak, Laurent Sifre, Morgane Rivière, Mihir Sanjay Kale, Juliette Love, Pouya Tafti, Léonard Hussenot, Pier Giuseppe Sessa, Aakanksha Chowdhery, Adam Roberts, Aditya Barua, Alex Botev, Alex Castro-Ros, Ambrose Slone, Amélie Héliou, Andrea Tacchetti, Anna Bulanova, Antonia Paterson, Beth Tsai, Bobak Shahriari, Charline Le Lan, Christopher A. Choquette-Choo, Clément Crepy, Daniel Cer, Daphne Ippolito, David Reid, Elena Buchatskaya, Eric Ni, Eric Noland, Geng Yan, George Tucker, George-Christian Muraru, Grigory Rozhdestvenskiy, Henryk Michalewski, Ian Tenney, Ivan Grishchenko, Jacob Austin, James Keeling, Jane Labanowski, Jean-Baptiste Lespiau, Jeff Stanway, Jenny Brennan, Jeremy Chen, Johan Ferret, Justin Chiu, Justin Mao-Jones, Katherine Lee, Kathy Yu, Katie Millican, Lars Lowe Sjoesund, Lisa Lee, Lucas Dixon, Machel Reid, Maciej Mikuła, Mateo Wirth, Michael Sharman, Nikolai Chinaev, Nithum Thain, Olivier Bachem, Oscar Chang, Oscar Wahltinez, Paige Bailey, Paul Michel, Petko Yotov, Rahma Chaabouni, Ramona Comanescu, Reena Jana, Rohan Anil, Ross McIlroy, Ruibo Liu, Ryan Mullins, Samuel L Smith, Sebastian Borgeaud, Sertan Girgin, Sholto Douglas, Shree Pandya, Siamak Shakeri, Soham De, Ted Klimenko, Tom Hennigan, Vlad Feinberg, Wojciech Stokowiec, Yu-hui Chen, Zafarali Ahmed, Zhitao Gong, Tris Warkentin, Ludovic Peran, Minh Giang, Clément Farabet, Oriol Vinyals, Jeff Dean, Koray Kavukcuoglu, Demis Hassabis, Zoubin Ghahramani, Douglas Eck, Joelle Barral, Fernando Pereira, Eli Collins, Armand Joulin, Noah Fiedel, Evan Senter, Alek Andreev, and Kathleen Kenealy. Gemma: Open Models Based on Gemini Research and Technology, 2024. URL https://arxiv.org/abs/2403.08295. Version Number: 4.

Hippolyte Gisserot-Boukhlef, Manuel Faysse, Emmanuel Malherbe, Céline Hudelot, and Pierre Colombo. Towards trustworthy reranking: A simple yet effective abstention mechanism, 2024. URL https://arxiv.org/abs/2402.12997.

Edward J. Hu, Yelong Shen, Phillip Wallis, Zeyuan Allen-Zhu, Yuanzhi Li, Shean Wang, Lu Wang, and Weizhu Chen. LoRA: Low-Rank Adaptation of Large Language Models. 2021. doi: 10.48550/ARXIV.2106.09685. URL https://arxiv.org/abs/2106.09685. Publisher: arXiv Version Number: 2.

Yupan Huang, Tengchao Lv, Lei Cui, Yutong Lu, and Furu Wei. LayoutLMv3: Pre-training for Document AI with Unified Text and Image Masking. 2022. doi: 10.48550/ARXIV.2204.08387. URL https://arxiv.org/abs/2204.08387. Publisher: arXiv Version Number: 3.

Albert Q. Jiang, Alexandre Sablayrolles, Arthur Mensch, Chris Bamford, Devendra Singh Chaplot, Diego de las Casas, Florian Bressand, Gianna Lengyel, Guillaume Lample, Lucile Saulnier, Lélio Renard Lavaud, Marie-Anne Lachaux, Pierre Stock, Teven Le Scao, Thibaut Lavril, Thomas Wang, Timothée Lacroix, and William El Sayed. Mistral 7B. 2023. doi: 10.48550/ARXIV.2310.06825. URL https://arxiv.org/abs/2310.06825. Publisher: arXiv Version Number: 1.

Ziyan Jiang, Rui Meng, Xinyi Yang, Semih Yavuz, Yingbo Zhou, and Wenhu Chen. Vlm2vec: Training vision-language models for massive multimodal embedding tasks, 2024. URL https://arxiv.org/abs/2410.05160.

Vladimir Karpukhin, Barlas Oğuz, Sewon Min, Patrick Lewis, Ledell Wu, Sergey Edunov, Danqi Chen, and Wen-tau Yih. Dense Passage Retrieval for Open-Domain Question Answering, 2020. URL https://arxiv.org/abs/2004.04906. Version Number: 3.

Omar Khattab and Matei Zaharia. ColBERT: Efficient and Effective Passage Search via Contextualized Late Interaction over BERT. 2020. doi: 10.48550/ARXIV.2004.12832. URL https://arxiv.org/abs/2004.12832.

Geewook Kim, Teakgyu Hong, Moonbin Yim, Jeongyeon Nam, Jinyoung Park, Jinyeong Yim, Wonseok Hwang, Sangdoo Yun, Dongyoon Han, and Seunghyun Park. OCR-free Document Understanding Transformer, 2021. URL https://arxiv.org/abs/2111.15664. Version Number: 5.

Andreas Koukounas, Georgios Mastrapas, Michael Günther, Bo Wang, Scott Martens, Isabelle Mohr, Saba Sturua, Mohammad Kalim Akram, Joan Fontanals Martínez, Saahil Ognawala, Susana Guzman, Maximilian Werk, Nan Wang, and Han Xiao. Jina CLIP: Your CLIP Model Is Also Your Text Retriever, 2024. URL https://arxiv.org/abs/2405.20204. Version Number: 1.

Hugo Laurençon, Andrés Marafioti, Victor Sanh, and Léo Tronchon. Building and better understanding vision-language models: insights and future directions., 2024a.

Hugo Laurençon, Léo Tronchon, Matthieu Cord, and Victor Sanh. What matters when building vision-language models?, May 2024b. URL http://arxiv.org/abs/2405.02246. arXiv:2405.02246 [cs].

Chankyu Lee, Rajarshi Roy, Mengyao Xu, Jonathan Raiman, Mohammad Shoeybi, Bryan Catanzaro, and Wei Ping. Nv-embed: Improved techniques for training llms as generalist embedding models, 2024. URL https://arxiv.org/abs/2405.17428.

Jinhyuk Lee, Zhuyun Dai, Sai Meher Karthik Duddu, Tao Lei, Iftekhar Naim, Ming-Wei Chang, and Vincent Y. Zhao. Rethinking the Role of Token Retrieval in Multi-Vector Retrieval, 2023. URL https://arxiv.org/abs/2304.01982. Version Number: 3.

Lei Li, Yuqi Wang, Runxin Xu, Peiyi Wang, Xiachong Feng, Lingpeng Kong, and Qi Liu. Multimodal arxiv: A dataset for improving scientific comprehension of large vision-language models, 2024.

Tsung-Yi Lin, Michael Maire, Serge Belongie, Lubomir Bourdev, Ross Girshick, James Hays, Pietro Perona, Deva Ramanan, C. Lawrence Zitnick, and Piotr Dollár. Microsoft COCO: Common Objects in Context, 2014. URL https://arxiv.org/abs/1405.0312. Version Number: 3.

Haotian Liu, Chunyuan Li, Qingyang Wu, and Yong Jae Lee. Visual Instruction Tuning. 2023. doi: 10.48550/ARXIV.2304.08485. URL https://arxiv.org/abs/2304.08485. Publisher: arXiv Version Number: 1.

Lucas Beyer*, Andreas Steiner*, André Susano Pinto*, Alexander Kolesnikov*, Xiao Wang*, Xiaohua Zhai*, Daniel Salz, Maxim Neumann, Ibrahim Alabdulmohsin, Michael Tschannen, Jeremiah Harmsen, Daniel Keysers, Neil Houlsby, Xi Chen, Emanuele Bugliarello, Thomas Unterthiner, Keran Rong, Matthias Minderer, Ioana Bica, Ivana Balazevic, Joan Puigcerver, Julian Eisenschlos, Manoj Kumar, Matko Bošnjak, Matthias Bauer, Fangyu Liu, Adam Grycner, Alexey Gritsenko, Paul Voigtlaender, Pinelopi Papalampidi, Olivier Henaff, Skanda Koppula, Xi Xiong, Radu Soricut, Model release contributors and general support, Tris Warkentin, Kat Black, Luiz Gustavo Martins, Glenn Cameron, Raj Gundluru, Manvinder Singh, Meg Risdal, Nilay Chauhan, Nate Keating, Nesh Devanathan, Elisa Bandy, Joe Fernandez, Antonia Paterson, Jenny Brennan, Tom Eccles, Pankil Botadra, Ben Bariach, Lav Rai, Minwoo Park, Dustin Luong, Daniel Vlasic, Bo Wu, Wenming Ye, Divyashree Sreepathihalli, Kiranbir Sodhia, Alek Andreev, Armand Joulin, Surya Bhupatiraju, Minh Giang, Joelle Barral, and Zoubin Ghahramani. PaliGemma, 2024. URL https://www.kaggle.com/m/23393.

Yubo Ma, Yuhang Zang, Liangyu Chen, Meiqi Chen, Yizhu Jiao, Xinze Li, Xinyuan Lu, Ziyu Liu, Yan Ma, Xiaoyi Dong, Pan Zhang, Liangming Pan, Yu-Gang Jiang, Jiaqi Wang, Yixin Cao, and Aixin Sun. Mmlongbench-doc: Benchmarking long-context document understanding with visualizations, 2024. URL https://arxiv.org/abs/2407.01523.

Minesh Mathew, Dimosthenis Karatzas, and C. V. Jawahar. DocVQA: A Dataset for VQA on Document Images. 2020. doi: 10.48550/ARXIV.2007.00398. URL https://arxiv.org/abs/2007.00398.

Minesh Mathew, Viraj Bagal, Rubèn Pérez Tito, Dimosthenis Karatzas, Ernest Valveny, and C. V Jawahar. InfographicVQA, 2021. URL https://arxiv.org/abs/2104.12756. Version Number: 2.

Niklas Muennighoff, Nouamane Tazi, Loïc Magne, and Nils Reimers. MTEB: Massive Text Embedding Benchmark, 2022. URL https://arxiv.org/abs/2210.07316. Version Number: 3.

Nomic. Nomic Embed Vision: Expanding The Nomic Latent Space, June 2024. URL https://blog.nomic.ai/posts/nomic-embed-vision.

Averi Nowak, Francesco Piccinno, and Yasemin Altun. Multimodal chart retrieval: A comparison of text, table and image based approaches. In Kevin Duh, Helena Gomez, and Steven Bethard (eds.), *Proceedings of the 2024 Conference of the North American Chapter of the Association for Computational Linguistics: Human Language Technologies (Volume 1: Long Papers)*, pp. 5488–5505, Mexico City, Mexico, June 2024. Association for Computational Linguistics. doi: 10.18653/v1/2024.naacl-long.307. URL https://aclanthology.org/2024.naacl-long.307.

Alec Radford, Jong Wook Kim, Chris Hallacy, Aditya Ramesh, Gabriel Goh, Sandhini Agarwal, Girish Sastry, Amanda Askell, Pamela Mishkin, Jack Clark, Gretchen Krueger, and Ilya Sutskever. Learning Transferable Visual Models From Natural Language Supervision. 2021. doi: 10.48550/ARXIV.2103.00020. URL https://arxiv.org/abs/2103.00020. Publisher: arXiv Version Number: 1.

Nils Reimers and Iryna Gurevych. Sentence-BERT: Sentence Embeddings using Siamese BERT-Networks, 2019. URL https://arxiv.org/abs/1908.10084. Version Number: 1.

Stephen E. Robertson, Steve Walker, Susan Jones, Micheline Hancock-Beaulieu, and Mike Gatford. Okapi at TREC-3. In Donna K. Harman (ed.), *Proceedings of The Third Text REtrieval Conference, TREC 1994, Gaithersburg, Maryland, USA, November 2-4, 1994*, volume 500-225 of *NIST Special Publication*, pp. 109–126. National Institute of Standards and Technology (NIST), 1994. URL http://trec.nist.gov/pubs/trec3/papers/city.ps.gz.

Keshav Santhanam, Omar Khattab, Christopher Potts, and Matei Zaharia. PLAID: An Efficient Engine for Late Interaction Retrieval, 2022. URL https://arxiv.org/abs/2205.09707. Version Number: 1.

R. Smith. An Overview of the Tesseract OCR Engine. In *Ninth International Conference on Document Analysis and Recognition (ICDAR 2007) Vol 2*, pp. 629–633, Curitiba, Parana, Brazil, September 2007. IEEE. ISBN 978-0-7695-2822-9. doi: 10.1109/ICDAR.2007.4376991. URL http://ieeexplore.ieee.org/document/4376991/. ISSN: 1520-5363.

Karen Sparck Jones. A STATISTICAL INTERPRETATION OF TERM SPECIFICITY AND ITS APPLICATION IN RETRIEVAL. *Journal of Documentation*, 28(1):11–21, January 1972. ISSN 0022-0418. doi: 10.1108/eb026526. URL https://www.emerald.com/insight/content/doi/10.1108/eb026526/full/html.

Zineng Tang, Ziyi Yang, Guoxin Wang, Yuwei Fang, Yang Liu, Chenguang Zhu, Michael Zeng, Cha Zhang, and Mohit Bansal. Unifying Vision, Text, and Layout for Universal Document Processing, 2022. URL https://arxiv.org/abs/2212.02623. Version Number: 3.

Nandan Thakur, Nils Reimers, Andreas Rücklé, Abhishek Srivastava, and Iryna Gurevych. BEIR: A Heterogenous Benchmark for Zero-shot Evaluation of Information Retrieval Models, 2021. URL https://arxiv.org/abs/2104.08663. Version Number: 4.

Ashish V. Thapliyal, Jordi Pont-Tuset, Xi Chen, and Radu Soricut. Crossmodal-3600: A Massively Multilingual Multimodal Evaluation Dataset, 2022. URL https://arxiv.org/abs/2205.12522. Version Number: 2.

Liang Wang, Nan Yang, Xiaolong Huang, Binxing Jiao, Linjun Yang, Daxin Jiang, Rangan Majumder, and Furu Wei. Text Embeddings by Weakly-Supervised Contrastive Pre-training, 2022. URL https://arxiv.org/abs/2212.03533. Version Number: 2.

Liang Wang, Nan Yang, Xiaolong Huang, Linjun Yang, Rangan Majumder, and Furu Wei. Improving text embeddings with large language models, 2024a. URL https://arxiv.org/abs/2401.00368.

Peng Wang, Shuai Bai, Sinan Tan, Shijie Wang, Zhihao Fan, Jinze Bai, Keqin Chen, Xuejing Liu, Jialin Wang, Wenbin Ge, Yang Fan, Kai Dang, Mengfei Du, Xuancheng Ren, Rui Men, Dayiheng Liu, Chang Zhou, Jingren Zhou, and Junyang Lin. Qwen2-vl: Enhancing vision-language model's perception of the world at any resolution, 2024b. URL https://arxiv.org/abs/2409.12191.

Wenhui Wang, Furu Wei, Li Dong, Hangbo Bao, Nan Yang, and Ming Zhou. MiniLM: Deep Self-Attention Distillation for Task-Agnostic Compression of Pre-Trained Transformers, April 2020. URL http://arxiv.org/abs/2002.10957. arXiv:2002.10957 [cs].

Lewei Yao, Runhui Huang, Lu Hou, Guansong Lu, Minzhe Niu, Hang Xu, Xiaodan Liang, Zhenguo Li, Xin Jiang, and Chunjing Xu. FILIP: Fine-grained Interactive Language-Image Pre-Training, 2021. URL https://arxiv.org/abs/2111.07783. Version Number: 1.

Xiang Yue, Yuansheng Ni, Kai Zhang, Tianyu Zheng, Ruoqi Liu, Ge Zhang, Samuel Stevens, Dongfu Jiang, Weiming Ren, Yuxuan Sun, Cong Wei, Botao Yu, Ruibin Yuan, Renliang Sun, Ming Yin, Boyuan Zheng, Zhenzhu Yang, Yibo Liu, Wenhao Huang, Huan Sun, Yu Su, and Wenhu Chen. MMMU: A Massive Multi-discipline Multimodal Understanding and Reasoning Benchmark for Expert AGI, 2023. URL https://arxiv.org/abs/2311.16502. Version Number: 3.

Xiaohua Zhai, Basil Mustafa, Alexander Kolesnikov, and Lucas Beyer. Sigmoid Loss for Language Image Pre-Training. 2023. doi: 10.48550/ARXIV.2303.15343. URL https://arxiv.org/abs/2303.15343. Publisher: [object Object] Version Number: 4.

Li Zhang, Shuo Zhang, and Krisztian Balog. Table2vec: Neural word and entity embeddings for table population and retrieval. In *Proceedings of the 42nd International ACM SIGIR Conference on Research and Development in Information Retrieval*, SIGIR '19. ACM, July 2019. doi: 10.1145/3331184.3331333. URL http://dx.doi.org/10.1145/3331184.3331333.

Ruochen Zhao, Hailin Chen, Weishi Wang, Fangkai Jiao, Xuan Long Do, Chengwei Qin, Bosheng Ding, Xiaobao Guo, Minzhi Li, Xingxuan Li, and Shafiq Joty. Retrieving Multimodal Information for Augmented Generation: A Survey, 2023. URL https://arxiv.org/abs/2303.10868. Version Number: 3.

Fengbin Zhu, Wenqiang Lei, Fuli Feng, Chao Wang, Haozhou Zhang, and Tat-Seng Chua. Towards Complex Document Understanding By Discrete Reasoning. 2022. doi: 10.48550/ARXIV.2207.11871. URL https://arxiv.org/abs/2207.11871. Publisher: arXiv Version Number: 3.

A BENCHMARK DATASETS

A.1 ACADEMIC DATASETS

DocVQA (Mathew et al., 2020) includes collected images from the UCSF Industry Documents Library. Questions and answers were manually annotated.

InfoVQA (Mathew et al., 2021) includes infographics collected from the Internet using the search query "*infographics*". Questions and answers were manually annotated.

TAT-DQA (Zhu et al., 2022) is a large-scale Document VQA dataset that was constructed from publicly available real-world financial reports. It focuses on rich tabular and textual content requiring numerical reasoning. Questions and answers were manually annotated by human experts in finance.

arXivQA (Li et al., 2024) is a VQA dataset based on figures extracted from arXiv publications. The questions were generated synthetically using GPT-4 Vision.

TabFQuAD (Table French Question Answering Dataset) is designed to evaluate TableQA models in realistic industry settings. We create additional queries to augment the existing human-annotated ones using the same method described in subsection A.2.

A.2 PRACTICAL DATASETS

Methodology. Creating a relevant retrieval dataset close to real use cases is a major challenge as the dataset needs to be both sufficiently large for effective fine-tuning and sufficiently diverse to cover a broad range of modalities (full text, tables, charts, ...), domains (industry, healthcare, ...), and query-document interactions (extractive questions, open-ended questions, ...). Our approach to building this dataset involves several steps: (1) we use a web crawler to collect publicly available documents on various themes and sources, (2) we convert these PDFs into a series of images, one per page, and (3) we generate queries related to each image using a VLM.

Web-Crawler. We implemented a web crawler to efficiently collect large volumes of documents related to a given topic. The crawler is seeded with a user-defined query (e.g. "artificial intelligence") and then uses GPT-3.5 Turbo to brainstorm related topics and subtopics. This query augmentation strategy aims at both broadening and deepening the search. GPT-3.5 Turbo is further used to generate diverse search queries from each subtopic. This query set is then consumed by a pool of parallel workers whose job is to fetch the associated most relevant documents. We use SerpAPI[17] along with a filetype filter (PDF documents only) to programmatically scrape Google Search rankings. Each file is hashed and stored in a Bloom filter (Bloom, 1970) shared among workers to avoid duplicate documents in the final corpus. Unique scraped files are downloaded, and inserted into a SQLite database along with additional metadata.

Datamix. Using the web crawler, we collected approximately 100 documents for each of the following four seeds: *"energy"*, *"government reports"*, *"healthcare industry"*, and *"artificial intelligence"*. These seeds were meticulously hand-picked to align with real-use cases for retrieval models and visually rich pages. We also removed all documents containing any private information.

Query Generation. To increase the efficiency of our query generation scheme and to limit API calls, we generate at most 3 questions per image. From all the documents collected, we randomly sample 10,000 images per theme and call Claude-3 Sonnet with the following prompt:

[17] https://serpapi.com/

```
You are an assistant specialized in Multimodal RAG tasks.

The task is the following: given an image from a pdf page, you will have to
generate questions that can be asked by a user to retrieve information from
a large documentary corpus.
The question should be relevant to the page, and should not be too specific
or too general. The question should be about the subject of the page, and
the answer needs to be found in the page.

Remember that the question is asked by a user to get some information from a
large documentary corpus that contains multimodal data. Generate a question
that could be asked by a user without knowing the existence and the content
of the corpus.
Generate as well the answer to the question, which should be found in the
page. And the format of the answer should be a list of words answering the
question.
Generate at most THREE pairs of questions and answers per page in a dictionary
with the following format, answer ONLY this dictionary NOTHING ELSE:

{
    "questions": [
        {
            "question": "XXXXXX",
            "answer": ["YYYYYY"]
        },
        {
            "question": "XXXXXX",
            "answer": ["YYYYYY"]
        },
        {
            "question": "XXXXXX",
            "answer": ["YYYYYY"]
        },
    ]
}
where XXXXXX is the question and ['YYYYYY'] is the corresponding list of answers
that could be as long as needed.

Note: If there are no questions to ask about the page, return an empty list.
Focus on making relevant questions concerning the page.
Here is the page:
```

Human Validation. We manually validate every single synthetically created query in *ViDoRe* to ensure quality, query relevance, and consistency with the benchmark objective of evaluating retrieval in practical industrial settings. During this step, we randomly assign document-pair queries to 4 volunteer annotators and instruct them to filter out queries that do not fit the above-listed criteria. We also instruct annotators to flag any documents they deem to contain PII information or content not suited for an academic benchmark. No flag was raised during the entirety of the process, validating our prior PDF collection strategy. 100 queries per topic are collected in this manner. Annotators are colleagues and collaborators of the authors who volunteered to help. Each annotator spent approximately 3 hours filtering the larger query set down to 100 high-quality queries per topic.

A.3 Training Dataset

The statistics of the train set are given in the following table. The creation of the train set follows the same methodology as in subsection A.2. We made sure that a PDF document cannot have pages in both the training set and the test set to prevent data leakage and that there are no duplicate documents in each split.

Dataset Split	Split Size	Language	Domain
DocVQA	39,463	English	Scanned documents from UCSF Industry
InfoVQA	10,074	English	Infographics scrapped from the web
TATDQA	13,251	English	High-quality financial reports
arXivQA	10,000	English	Scientific Scientific Figures from arXiv
Scrapped PDFs	45,940	English	Varied PDFs from 3885 distinct URL domains
TOTAL	**118,695**	**English-only**	**Mixed**

Table 3: Details on the different splits in the dataset used to train ColPali.

B Implementation details

B.1 Codebase

The codebase is written in PyTorch[18] and leverages HuggingFace tooling for model implementations and trainers[19].

B.2 Hyperparameters

Hyperparameters are tuned on a validation split composed of 2% of the training dataset. We find bi-encoder methods to be more sensible to learning rate variations than late interaction-based models and achieve the best performance for all models with a learning rate of $5e-5$. We experiment with LoRA rank and α values and do not notice particular improvements past $r = \alpha = 32$. Per-device batch sizes are kept small due to long sequence lengths that complicate scaling past $b = 4$. We simulate larger batch sizes with multi-GPU training and train with a total batch size $b = 32$ with no accumulation, for 1 epoch on our training set.

B.3 Embedding size

Minimizing storage footprint can be essential to industrial retrieval systems if databases contain millions of documents. With this criterion in view, we have compared the embedding sizes of the models in our study. As shown in Table 4, *ColPali*'s embedding size is an order of magnitude larger than BM25 and two orders of magnitude larger than BGE-M3. However, in practical scenarios, pooling multi-vector embeddings by centroid cluster, or quantizing embeddings to binary representations [20] can reduce storage costs by two orders of magnitude (Santhanam et al., 2022) with minimal performance hits, and make storage costs competitive with other systems.

Model	Embedding size (KB)
BGE-M3	8.60
BM25 (dense emb.)	3.00
BM25 (sparse emb.)	1.56 ± 0.51
ColPali (float16)	257.5

Table 4: Comparison of the embedding sizes for the DocVQA test set from *ViDoRe* w.r.t. different retrieval models. The *mean* ± *std* size is given for the sparse embeddings. In general multiple vectors (2-5) per page are used for BGE-M3 and BM25.

B.4 Latency computations

To ensure comparison fairness, the latencies of the different retrieval systems shown in Figure 2 are measured on the same `g2-standard-8` GCP VM with a NVIDIA L4 GPU. Document pages are embedded using the highest settings of `Unstructured` with captioning (see subsection 3.2). SigLIP and *ColPali* are both loaded with `bfloat16` parameter dtypes. The reported times in Table 5 are the

[18] `https://pytorch.org/`

[19] `https://huggingface.co`

[20] `https://blog.vespa.ai/scaling-colpali-to-billions/`

average per-page latencies for each indexing operation on 1000 randomly chosen documents across all splits of the *ViDoRe* benchmark test set. A batch size of 8 was used for the BGE-M3 model used with `Unstructured`, and a batch size of 4 was used for SigLIP and *ColPali*.

Indexing operation	**Latency (s)**		
	Unstructured	**SigLIP**	***ColPali***
Layout detection	0.81	NA	NA
OCR	2.67	NA	NA
Captioning	3.71	NA	NA
Page encoding	0.03	0.12	0.39
Total	7.22	0.12	0.39

Table 5: Page-level latencies for document indexing using various retrieval systems. SigLIP and *ColPali* are much faster than `Unstructured` because they don't require the layout detection, OCR, and captioning operations.

B.5 CAPTIONING

Examples of captions generated for visually rich document chunks with Claude-3 Sonnet are shown in Figure 5 and Figure 4. The prompt used for generating the description is the following:

> You are an assistant specialized in document analysis. Given a table or a figure, you have to provide a detailed summary of the content in maximum 3000 characters. Your summary should be qualitative and not quantitative. Here is the table/figure to analyze: {image}. Answer ONLY with the caption of the table/figure.

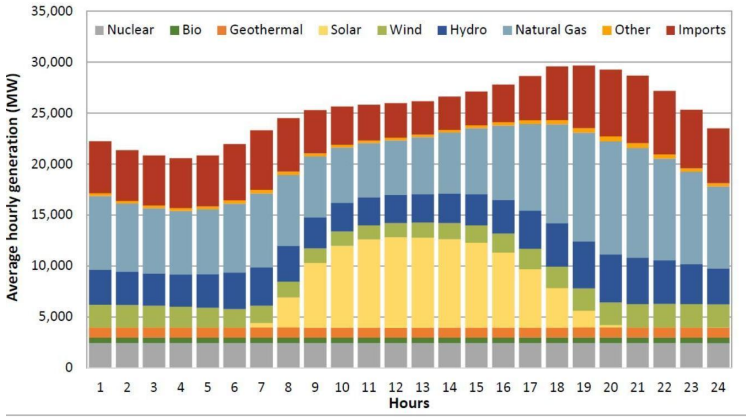

Figure 4: Example from the "Energy" test set.
Caption: *The image depicts the hourly energy generation profile, illustrating the contributions of various energy sources over 24 hours. The data is presented as a stacked bar chart, with the x-axis representing the hours of the day from 1 to 2, and the y-axis showing the average hourly generation in MW. The bars are segmented into different colors, each representing a distinct energy source: nuclear, bio, geothermal, solar, wind, hydro, natural gas, and other imports. The chart provides insights into the temporal variations in energy generation across different sources, highlighting the interplay between baseload and intermittent sources throughout the day.*

Document	System of Record[1]									
	County Servers		*Project View*		*OnBase*		*CGI Advantage Financial System*		*Purchasing Department*	
Project plan/scope	W	T								
Project budgets	W	T	W	T						
Schedules/timeline (design)	W	T	W	T		T				
Schedules/timeline (construction)	W	T	W							
Executed contracts		T			W	T			W	T
Purchase orders		T			W				W	T
Solicitation advertisements		T			W	T			W	T
Proposal submissions		T			W				W	T
Selection committee evaluation documents		T			W	T			W	T
Independent cost estimates		T	W	T	W	T			W	
Negotiation details		T			W				W	
Notice of award		T			W				W	
Notice to proceed		T			W				W	
Invoices/applications for payment ("AFP")			W	T	W		W	T		
Change order requests		T			W					
Approved change orders		T	W	T	W					
Requests for Information (RFI)	W	T							W	T
Bid submissions					W				W	T
Shop drawings	W	T				T				
Photographs	W	T								
As-builts	W	T				T				
Operating manuals	W	T								
Maintenance schedules	W	T								
Warranties	W	T				T				
Daily diaries	N/A	T								
Weekly meeting minutes	W	T								
Monthly progress reports	W	T								
Allowance usage logs	W	T								
Punch lists	W	T								
Insurance records		T			W					

Figure 5: Example from the "Government Reports" test set.
Caption: *The image shows a table titled "System of Record" which outlines the different types of documents or records maintained across various systems or departments within an organization related to project management and construction. The rows list documents like project plans, budgets, schedules, contracts, purchase orders, invoices, change requests, bid submissions, drawings, manuals, meeting minutes, and reports. The columns indicate the system or department responsible for maintaining each record, such as County Servers, Project View, OnBase, CGI Advantage Financial System, and Purchasing Department. The table uses "W" and "T" markers to denote which system or department serves as the primary source (writer) or storage location (trailer) for each type of document.*

C ADDITIONAL RESULTS

C.1 OTHER METRICS

	ArxivQ	DocQ	InfoQ	TabF	TATQ	Shift	AI	Energy	Gov.	Health.	Avg.
Unstructured text-only											
BM25	-	26.6	-	-	34.6	45.0	86.0	70.0	68.0	74.0	-
BGE-M3	-	22.8$_{\downarrow 3.8}$	-	-	26.1$_{\downarrow 8.5}$	51.0$_{\uparrow 6.0}$	81.0$_{\downarrow 5.0}$	72.0$_{\uparrow 2.0}$	67.0$_{\downarrow 1.0}$	77.0$_{\uparrow 3.0}$	-
Unstructured + OCR											
BM25	26.7	28.9	54.0	30.4	50.0	52.0	86.0	77.0	74.0	80.0	55.9
BGE-M3	28.1$_{\uparrow 1.4}$	22.9$_{\downarrow 6.0}$	53.8$_{\downarrow 0.2}$	55.7$_{\uparrow 25.3}$	38.6$_{\downarrow 11.4}$	**56.0**$_{\uparrow 4.0}$	82.0$_{\downarrow 4.0}$	79.0$_{\uparrow 2.0}$	76.0$_{\uparrow 2.0}$	83.0$_{\uparrow 3.0}$	57.5$_{\uparrow 1.6}$
Unstructured + Captioning											
BM25	35.5	30.2	61.5	24.3	49.0	47.0	79.0	76.0	75.0	81.0	55.9
BGE-M3	29.3$_{\downarrow 6.2}$	26.0$_{\downarrow 4.2}$	62.1 $_{\uparrow 0.6}$	58.6$_{\uparrow 34.3}$	30.6$_{\downarrow 18.4}$	55.0$_{\uparrow 8.0}$	80.0$_{\uparrow 1.0}$	78.0$_{\uparrow 2.0}$	69.0$_{\downarrow 6.0}$	83.0$_{\uparrow 2.0}$	57.2$_{\uparrow 1.3}$
Contrastive VLMs											
Jina-CLIP	19.4	7.3	26.7	12.5	1.6	2.0	11.0	13.0	15.0	17.0	12.6
Nomic-vision	10.4	6.7	22.1	9.6	1.6	0.0	9.0	9.0	7.0	13.0	8.8
SigLIP (Vanilla)	34.2	21.3	51.8	46.1	17.9	13.0	50.0	51.0	47.0	65.0	39.7
Ours											
SigLIP (Vanilla)	34.2	21.3	51.8	46.1	17.9	13.0	50.0	51.0	47.0	65.0	39.7
BiSigLIP (+fine-tuning)	49.2$_{\uparrow 15.0}$	23.8$_{\uparrow 2.5}$	59.0$_{\uparrow 7.2}$	52.1$_{\uparrow 6.0}$	20.7$_{\uparrow 2.8}$	16.0$_{\uparrow 3.0}$	62.0$_{\uparrow 12.0}$	61.0$_{\uparrow 10.0}$	55.0$_{\uparrow 8.0}$	72.0$_{\uparrow 7.0}$	47.1$_{\uparrow 7.4}$
BiPali (+LLM)	46.4$_{\downarrow -2.8}$	20.0$_{\downarrow -3.8}$	54.6$_{\downarrow -4.4}$	63.2$_{\uparrow 11.1}$	20.4$_{\downarrow -0.4}$	34.0$_{\uparrow 18.0}$	59.0$_{\downarrow -3.0}$	45.0$_{\downarrow -16.0}$	57.0$_{\uparrow 2.0}$	56.0$_{\downarrow -16.0}$	45.6$_{\downarrow -1.5}$
ColPali (+Late Inter.)	**72.4**$_{\uparrow 26.0}$	**45.6**$_{\uparrow 25.6}$	**74.6**$_{\uparrow 20.0}$	**75.4**$_{\uparrow 12.1}$	**53.1**$_{\uparrow 32.7}$	55.0$_{\uparrow 21.0}$	**93.0**$_{\uparrow 34.0}$	**85.0**$_{\uparrow 40.0}$	**85.0**$_{\uparrow 28.0}$	**88.0**$_{\uparrow 32.0}$	**72.7**$_{\uparrow 27.1}$

Table 6: **Comprehensive evaluation of baseline models and our proposed method on *ViDoRe*.** Results are presented using Recall@1 metrics. Text-only metrics are not computed for benchmarks with only visual elements.

C.2 MODEL VARIANTS

	ArxivQ	DocQ	InfoQ	TabF	TATQ	Shift	AI	Energy	Gov.	Health.	Avg.
ColSigLIP (PaliGemma)	3.1	3.0	5.1	6.2	2.5	1.0	3.4	3.4	2.3	2.2	3.2
BiSigLIP (PaliGemma)	18.5	14.6	33.4	39.5	16.1	5.2	27.6	32.6	36.6	35.7	26.0
ColSigLIP (Original)	2.6	2.2	2.3	5.7	1.8	1.0	2.6	4.1	1.4	1.5	2.5
ColPali (No Q.A. Tokens)	80.4	53.2	82.4	77.4	65.7	63.4	97.0	89.9	93.6	92.4	79.6
ColPali (Docmatix)	71.3	48.0	80.0	83.9	59.1	73.8	95.7	93.8	92.5	93.1	79.1
ColPali (224)	71.0	37.4	62.3	65.7	28.6	20.4	65.7	66.8	73.9	73.0	56.5
ColPali (Vision Trained)	78.8	53.9	81.3	81.7	64.4	70.6	95.3	91.7	93.5	94.7	80.6
ColPali (No Pairwise)	79.0	53.0	82.1	85.3	63.2	66.2	94.9	88.9	92.7	92.1	79.7
ColPali (+TabFQuAD training)	77.6	54.7	82.6	86.5	65.4	73.9	94.8	92.4	**94.2**	94.8	81.7
ColIdefics2 (64)	73.6	48.0	82.4	81.6	63.0	57.2	95.5	86.9	86.6	91.2	76.6
ColQwen2 (768)	**86.4**	**56.2**	**89.8**	**88.7**	**75.2**	**85.7**	**98.8**	**94.8**	93.6	**97.3**	**86.6**
ColPali (Reference: 448)	79.1	54.4	81.8	83.9	65.8	73.2	96.2	91.0	92.7	94.4	81.3

Table 7: **Benchmark scores for the "negative results" and various ablations on *ViDoRe*; *ColPali* for reference.** Results are presented using nDCG@5 metrics. Text-only metrics are not computed for benchmarks with only visual elements.

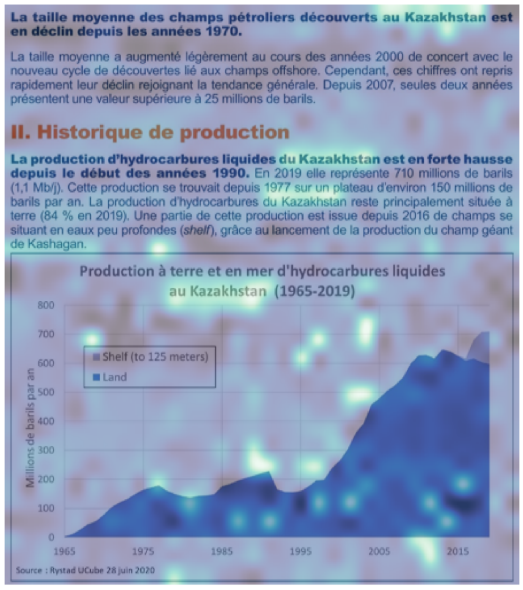

Query: "Quelle partie de la production pétrolière du Kazakhstan provient de champs en mer ?"

Figure 6: Similarity of the image patches w.r.t. the underlined token in the user query. This example is from the *Shift* test set.

D MORE SIMILARITY MAPS

In Figure 6, *ColPali* assigns a high similarity to all patches with the word *"Kazakhstan"* when given the token `<_Kazakhstan>`. Moreover, our model seems to exhibit world knowledge capabilities as the patch around the word *"Kashagan"*—an offshore oil field in Kazakhstan—also shows a high similarity score.

It is also interesting to highlight that both this similarity map and the one displayed in Figure 3 (right) showcase a few white patches with high similarity scores. This behavior might first seem surprising as the white patches should not carry a meaningful signal from the original images. We believe the vectors associated with these patches share a similar role with the ViT registers (Darcet et al., 2023), i.e. these patches were repurposed for internal computations and stored the global information from the whole image.

E MODEL GLOSSARY

SIGLIP

SigLIP (Sigmoid Loss for Language Image Pre-Training) builds upon CLIP (Contrastive Language-Image Pretraining)—a foundational model that aligns images and text by maximizing the similarity between correct image-text pairs while minimizing it for incorrect ones, leveraging a contrastive loss (Zhai et al., 2023). Unlike CLIP (Radford et al., 2021), which applies the softmax function to the logits, SigLIP uses the sigmoid activation function. This innovation eliminates the need for a global view of all pairwise similarities between images and texts within a batch, enabling more flexible batch size scaling (up to 1M items per batch, with an effective optimal batch size of 32k). This approach allows SigLIP to achieve state-of-the-art performance in zero-shot image classification tasks.

PALIGEMMA

PaliGemma is a 3B-parameter vision-language model. It integrates the SigLIP vision encoder with a Gemma-2B language decoder, connected via a multimodal linear projection layer (Lucas Beyer* et al.,

2024). The model processes images by segmenting them into a fixed number of Vision Transformer (Dosovitskiy et al., 2020) tokens, which are prepended to an optional text prompt.

A distinguishing feature of PaliGemma is its operation as a Prefix-Language Model (Prefix-LM). This design ensures full attention between image tokens and the user-provided input (prefix) while generating outputs auto-regressively (suffix). This architecture allows image tokens to access the task-specific query during processing, facilitating more effective task-dependent reasoning.

PaliGemma was trained in four stages: unimodal pretraining with existing components, extended multimodal pretraining, short high-resolution pretraining, and task-specific fine-tuning.

ColBERT

ColBERT (Contextualized Late Interaction over BERT) is a retrieval model designed to balance speed and effectiveness in information retrieval tasks (Khattab & Zaharia, 2020). Traditional retrieval models are typically categorized based on their type of interaction: either processing queries and documents independently for efficiency (bi-encoders) or jointly to capture rich contextual relationships (cross-encoders). ColBERT combines the advantages of both approaches through a novel late interaction mechanism.

Queries and documents are encoded separately using BERT, enabling offline pre-computation of document representations for scalability. Instead of pooling embeddings into a single vector, ColBERT retains token-level embeddings and employs a MaxSim operator to compute fine-grained similarity scores. For each query token, the model determines the maximum similarity with document tokens, summing these scores to compute relevance.

This architecture preserves the contextual richness of deep language models while significantly improving computational efficiency. By delaying the interaction step, ColBERT supports vector similarity indexing, facilitating end-to-end retrieval from large collections without prohibitive costs. Empirical evaluations on passage search datasets demonstrate that ColBERT achieves competitive effectiveness compared to existing BERT-based models (Devlin et al., 2018), while executing queries orders of magnitude faster and with drastically reduced computational requirements.

F EXAMPLES FROM THE *ViDoRe* BENCHMARK

Energy

Query: What types of accounts or products allow investors to defer paying taxes?

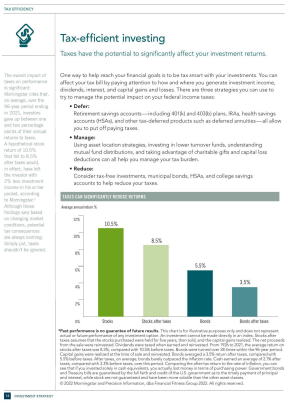

TAX EFFICIENCY

Tax-efficient investing

Taxes have the potential to significantly affect your investment returns.

The overall impact of taxes on performance is significant: Morningstar cites that, on average, over the 96-year period ending in 2021, investors lost 1.66 percentage point two percentage points of their annual returns to taxes. A hypothetical stock return of 10.0%, that fell to 8.0% after taxes would, in effect, have left investors with only 2% less investment income in his or her pocket, according to Morningstar.[1] Although these findings vary based on changing market conditions, potential investors should see always tantalizing. Simply put, "taxes shouldn't be ignored.

One way to help reach your financial goals is to be tax smart with your investments. You can affect your tax bill by paying attention to how and where you generate investment income, dividends, interest, and capital gains and losses. There are three strategies you can use to try to manage the potential impact on your federal income taxes:

- **Defer:**
  Retirement savings accounts—including 401(k) and 403(b) plans, IRAs, health savings accounts (HSAs), and other tax-deferred products such as deferred annuities—all allow you to put off paying taxes.
- **Manage:**
  Using asset location strategies, investing in lower turnover funds, understanding mutual fund distributions, and taking advantage of charitable gifts and capital loss deductions can all help you manage your tax burden.
- **Reduce:**
  Consider tax-free investments, municipal bonds, HSAs, and college savings accounts to help reduce your taxes.

TAXES CAN SIGNIFICANTLY REDUCE RETURNS

Average annualized %

*Past performance is no guarantee of future results. This chart is for illustrative purposes only and does not represent actual or future performance of any investment option. An investment cannot be made directly in an index. Stocks after taxes assumes that the stocks purchased were held for five years, then sold, and the capital gains realized. The net proceeds were then invested in the stocks of companies in the Standard & Poor's 500 Index (S&P 500). Bonds after taxes assumes that bonds after taxes was 3.5%, compared with 10.5% before taxes. Bonds were turned over 20 times which made the gains all Capital gains were realized at the time of sale and reinvested. Bonds averaged a 3.5% return after taxes, compared with 5.5% before taxes. At 25 tax-year average, bonds lately captured the inflation rate. Cash earnings averaged 2.1% after taxes, compared with 3.5% before taxes. Cash earnings were taxed at the ordinary income tax rate. Bonds are safe if you see that if you invested solely in cash equivalents, you actually lost money in terms of purchasing power. Government bonds and Treasury bills are guaranteed by the full faith and credit of the U.S. government as to the timely payment of principal and interest, and if held to maturity, offer a fixed rate of return and principal value that is guaranteed.

© 2022 Morningstar and Precision Information, dba Financial Fitness Group 2022. All rights reserved.

Query: What is the estimated total savings for a PV system in Durham under the net metering (flat rate) billing option over the system's useful life of 25 years?

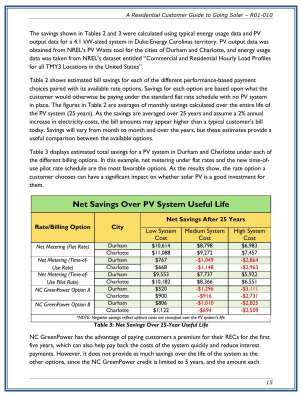

A Residential Customer Guide to Going Solar – R01-010

The savings shown in Tables 2 and 3 were calculated using typical energy usage data and PV output data for a 6.1 kW-sized system in Duke Energy Carolinas territory. PV output data was obtained from NREL's PV Watts tool for the cities of Durham and Charlotte, and energy usage data was taken from NREL's dataset entitled "Commercial and Residential Hourly Load Profiles for all TMY3 Locations in the United States".

Table 2 shows estimated bill savings for each of the different performance-based payment choices paired with its available rate options. Savings for each option are based upon what the customer would otherwise be paying under the standard flat rate schedule with no PV system in place. The figures in Table 2 are averages of monthly savings calculated over the entire life of the PV system (25 years). As the savings are averaged over 25 years and assume a 2% annual increase in electricity costs, the bill amounts may appear higher than a typical customer's bill today. Savings will vary from month to month and over the years, but these estimates provide a useful comparison between the available options.

Table 3 displays estimated total savings for a PV system in Durham and Charlotte under each of the different billing options. In this example, net metering under flat rates and the new time-of-use pilot rate schedule are the most favorable options. As the results show, the rate option a customer chooses can have a significant impact on whether solar PV is a good investment for them.

Net Savings Over PV System Useful Life

Rate/Billing Option	City	Net Savings After 25 Years		
		Low System Cost	Medium System Cost	High System Cost
Net Metering (Flat Rate)	Durham	$10,614	$8,798	$6,983
	Charlotte	$11,088	$9,273	$7,457
Net Metering (Time-of-Use Rate)	Durham	$760	-$1,004	-$2,864
	Charlotte	$668	-$1,148	-$3,963
Net Metering (Time-of-Use Pilot Rate)	Durham	$9,551	$7,737	$5,922
	Charlotte	$10,182	$8,366	$6,551
NC GreenPower Option A	Durham	$500	-$1,296	-$3,111
	Charlotte	$900	-$916	-$2,731
NC GreenPower Option B	Durham	$806	-$1,010	-$2,823
	Charlotte	$1,122	-$694	-$2,509

*NOTE: Negative savings reflect upfront costs not recouped over the 25-year period.

Table 3: *Net Savings Over 25-Year Useful Life*

NC GreenPower has the advantage of paying customers a premium for their RECs for the first five years, which can also help pay back the costs of the system quickly and reduce interest payments. However, it does not provide as much savings over the life of the system as the other options, since the NC GreenPower credit is limited to 5 years, and the amount each

Query: What is the projected peak electricity demand in California for the year 2030?

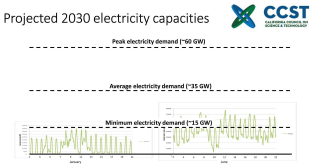

Artificial Intelligence

Query: What are some common outcome areas targeted by TAII for different age groups?

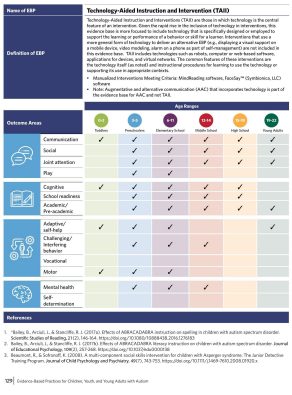

Name of EBP	Technology-Aided Instruction and Intervention (TAII)
Definition of EBP	Technology-Aided Instruction and Interventions (TAII) are those in which technology is the central feature of an intervention. Given the rapid rise in the inclusion of technology in interventions, this evidence base is more focused to include technology that is specifically designed or employed to teach a skill or behavior or to support the teaching of a skill or behavior. Technology-aided is a more general form of technology to deliver an alternative EBP (e.g., displaying a visual support on a mobile device, video modeling, alarm on a phone as part of self-management) are not included in this evidence base. TAII includes technologies such as robots, computer or web based software, applications for devices, and virtual networks. The common features of these interventions are technology is the central feature of the intervention and instructional procedures for learning to use the technology or supporting its use in appropriate contexts. • Manualized Interventions Meeting Criteria: MindReading software, FaceSay™ (Symbionics, LLC) software • Note: Augmentative and alternative communication (AAC) that incorporates technology is part of the evidence base for AAC and not TAII.

Outcome Areas		Age Ranges: 0-2 Toddlers	3-5 Preschoolers	6-11 Elementary School	12-14 Middle School	15-18 High School	19-22 Young Adults
Communication	Communication	✓	✓	✓	✓	✓	✓
	Social		✓	✓	✓	✓	✓
	Joint attention		✓	✓	✓	✓	✓
	Play		✓	✓			
Cognitive	Cognitive	✓	✓	✓	✓	✓	
	School readiness		✓	✓	✓	✓	
	Academic/ Pre-academic		✓	✓	✓	✓	✓
Adaptive/ self-help	Adaptive/ self-help	✓	✓	✓			✓
	Challenging/ Interfering behavior		✓	✓	✓		
	Vocational						
	Motor	✓	✓	✓			
Mental health	Mental health		✓	✓	✓		
Self-determination	Self-determination						

References

1. *Boileau, B., Arciuli, J., & Stancliffe, R. J. (2021a). Effects of ABRACADABRA intervention on spelling in children with autism spectrum disorder. Scientific Studies of Reading, 21(2), 146-164. https://doi.org/10.1080/10888438.2016.1276083*
2. *Bailey, B., Arciuli, J., & Stancliffe, R. J. (2021b). Effects of ABRACADABRA literacy intervention on children with autism spectrum disorder. Journal of Educational Psychology, 109(2), 257-268. https://doi.org/10.1037/edu0000538*
3. *Beaumont, R., & Sofronoff, K. (2008). A multi-component social skills intervention for children with Asperger syndrome: The Junior Detective Training Program. Journal of Child Psychology and Psychiatry, 49(7), 743-753. https://doi.org/10.1111/j.1469-7610.2008.01920.x*

Query: What did the robot monitor to determine when to activate or deactivate the blower motor and blinker?

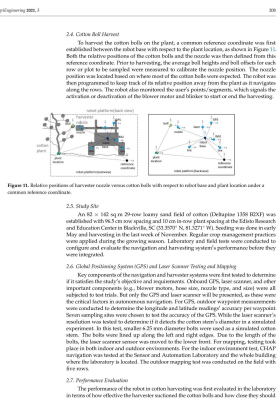

AgriEngineering 2021, *3* 306

2.4. Cotton Bolll Harvest

To harvest the cotton bolls on the plant, a common reference coordinate was first established between the robot base with respect to the plant location, as shown in Figure 11. Both the relative positions of the cotton bolls and the nozzle was then defined from this reference coordinate. Prior to harvesting, the average boll heights and boll offsets for each row or plot to be sampled were measured to calibrate the nozzle position. The nozzle position was located based on where most of the cotton bolls were expected. The robot was then programmed to keep track of its relative position away from the plant as it navigates along the rows. The robot also monitored the user's points/segments, which signals the activation or deactivation of the blower motor and blinker to start or end the harvesting.

Figure 11. Relative positions of harvester nozzle versus cotton bolls with respect to robot base and plant location under a common reference coordinate.

2.5. Study Site

An 82 × 142 sq. m 29-row loamy sand field of cotton (Deltapine 1358 B2XF) was established with 96.5 cm row spacing and 10 cm in-row plant spacing at the Edisto Research and Education Center in Blackville, SC (33.3597° N, 81.3271° W). Seeding was done in early May and harvesting in the last week of November. Regular crop management practices were applied during the growing season. Laboratory and field tests were conducted to configure and evaluate the navigation and harvesting system's performance before they were integrated.

2.6. Global Positioning System (GPS) and Laser Scanner Testing and Mapping

Key components of the navigation and harvester systems were first tested to determine if it satisfies the study's objective and requirements. Onboard GPS, laser scanner, and other important components (e.g., blower motors, hose size, nozzle type, and size) were all subjected to test trials. But only the GPS and laser scanner will be presented, as these were the critical factors in autonomous navigation. For GPS, outdoor waypoint measurements were conducted to determine the longitude and latitude readings' accuracy per waypoint. Seven sampling sites were chosen to test the accuracy of the GPS. While the laser scanner's resolution was tested to determine if it detects the cotton stem's diameter in a simulated experiment. In this test, smaller 8.25 mm diameter bolts were used as a simulated cotton stem. The bolts were lined up along the left and right edges. Due to the length of the bolts, the laser scanner sensor was moved to the lower front. For mapping, testing took place in both indoor and outdoor environments. For the indoor environment test, CIAAP navigation was tested at the Sensor and Automation Laboratory and the whole building where the laboratory is located. The outdoor mapping test was conducted on the field with five rows.

2.7. Performance Evaluation

The performance of the robot in cotton harvesting was first evaluated in the laboratory in terms of how effective the harvester suctioned the cotton bolls and how close they should

Query: What is the key approach used in the PDP architecture?

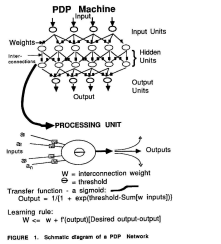

FIGURE 1. Schmatic diagram of a PDP Network

A key approach in the PDP architecture is the use of an adaptive filter. The adaptive filter can accept a real-world analog input and compare it to a stored pattern. The stored pattern represents the desired input level which can then be modified as necessary so that echo-free signals can be produced the correct results. A more abstract argument driving the design of the PDP network is machine efficiency, that is, the optimal utilization of the total computer circuitry. In the more familiar structure of a modern computer (the von Neumann architecture) most of the computer's circuitry in the memory is not in active use most of the time. This is very wasteful from a pure resource management standpoint. The PDP machine addresses this problem by using many processors and memories, but does so

Healthcare Industry

Query: What is the chemical formula for the ferroelectric material Lead Zirconium Titanate (PZT)?

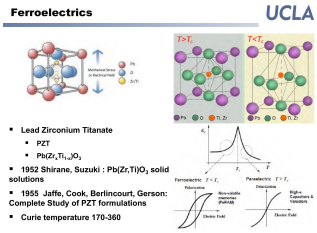

Query: What government entities are involved in public financing for healthcare in the US?

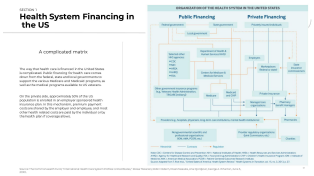

Query: What does the AVPU scale stand for in assessing the level of consciousness of a seriously ill child?

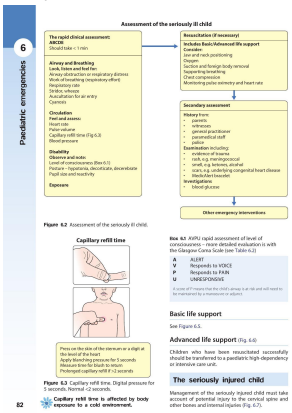

Government Reports

Query: What are some mandates for the EPA under the Pollution Prevention Act?

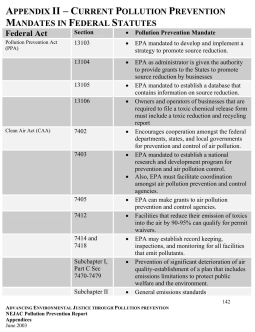

Query: What is the strategy of KPMG Hazem Hassan?

Query: What is the trust signal score for the consumer industry best-in-class archetype?

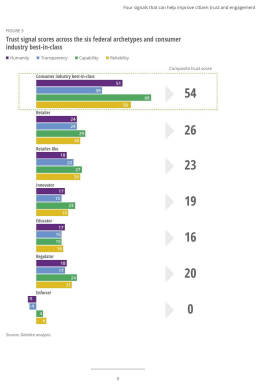

Shift

Query: Selon le graphique, quelle est la capacité d'import et la consommation réelle de carburants SAF (biocarburants durables pour l'aviation) prévues en 2050 ?

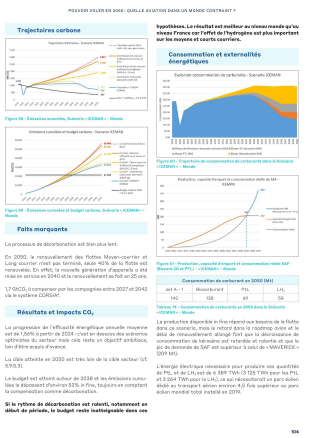

Query: Quelle partie de la production pétrolière du Kazakhstan provient de champs en mer ?

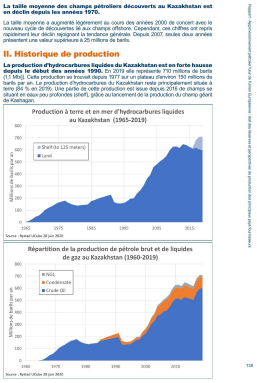
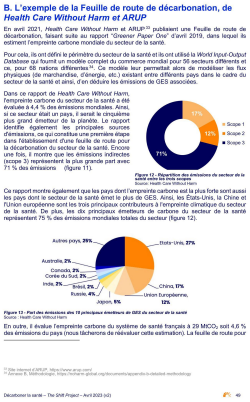
Query: Quels sont les pays ayant la plus grande part des découvertes cumulées de pétrole brut en 2020 (en milliers de barils, hors découvertes cumulées) ?